



# Characterization of trace gas emissions from controlled laboratory burning of Canadian boreal forest fuels

Rowshon Afroz<sup>1</sup>, Hongru Shen<sup>2,3</sup>, Bradley H. Isenor<sup>2</sup>, Samar G. Moussa<sup>4</sup>, Amanda Hanashiro Moraes<sup>1</sup>, Shakiba Talebian<sup>1</sup>, Carolyn Liu-Kang<sup>2</sup>, Jeremy J. B. Wentzell<sup>4</sup>, Oscar Olfert<sup>5</sup>, Amy Leithead<sup>4</sup>, Ginny Marshall<sup>6</sup>, Ralf M. Staebler<sup>4</sup>, Cris Mihele<sup>4</sup>, Arthur W. H. Chan<sup>7</sup>, Jason Olfert<sup>5</sup>, John Liggio<sup>3</sup>, Jonathan Abbatt<sup>2</sup>, Ran Zhao<sup>1</sup>, and Sumi N. Wren<sup>4</sup>

<sup>1</sup>Department of Chemistry, University of Alberta, Edmonton, Alberta, Canada

<sup>2</sup>Department of Chemistry, University of Toronto, Toronto, Ontario, Canada

<sup>3</sup>School of Environmental Science and Engineering, Shanghai Jiao Tong University, Shanghai, China

<sup>4</sup>Air Quality Research Division, Environment and Climate Change Canada, Toronto, Ontario, Canada

<sup>5</sup>Department of Mechanical Engineering, University of Alberta, Edmonton, Alberta, Canada

<sup>6</sup>Natural Resources Canada, Edmonton, Alberta, Canada

<sup>7</sup>Department of Chemical Engineering and Applied Chemistry, University of Toronto, Toronto, Ontario, Canada

**Correspondence:** Sumi N. Wren (sumi.wren@ec.gc.ca)

**Abstract.** Although boreal wildfires are a major global source of trace gases, their emissions remain poorly characterized. To address this gap, controlled burns of Canadian Boreal surface and ground fuels were conducted during the Biomass Burning Canada (BBCan) Campaign. Emission factors (EF) for 46 volatile organic compounds (VOC) were determined using iodide chemical ionization mass spectrometry (I-CIMS) and Vocus proton transfer reaction mass spectrometry (Vocus PTR-MS). Total non-methane organic compound (NMOC) emissions, which were measured separately, were found to account for 1–13 % of total emitted gas-phase carbon (i.e., CO<sub>2</sub>, CO, CH<sub>4</sub>, NMOC), with total quantified VOCs ( $\sum$  VOCs) accounting for 13–34 % of that fraction. The dominant compounds contributing to the measured  $\sum$  VOCs include oxygenates and organic reactive nitrogen (Nr) species. Boreal peat fuels, which are prone to residual smoldering combustion, produced significantly higher total NMOC, total Nr, and individual VOC emissions than the other fuels. In contrast, boreal mulch, which burned very efficiently, produced low emissions. Combustion efficiency was observed to have a strong impact on total and individual VOC emissions, but VOC emission profiles were also dependent on fuel type and moisture content. The findings indicate that the EFs currently used to speciate NMOC emission may not adequately capture emissions from smoldering boreal peat fires. Study results provide the first comprehensive VOC EF for fresh emissions for a range of Canadian boreal surface and ground fuels, which can be used to improve emission inventories and enhance predictions of wildfire smoke impacts on air quality, climate, and health.

## 1 Introduction

Canada, with 28 % of the world's boreal forest (552 million ha) and 9 % of the world's forests, has experienced a long history of wildfire activity that varies significantly by region and season (Natural Resources Canada, 2025a; Chen et al., 2019). Over



the previous decade, the country experienced an average of 7,000 wildfires annually, burning about 2.6 million hectares each  
20 year (Canadian Interagency Forest Fire Centre, 2017). However, as a result of climate change-driven droughts and higher  
temperatures (Abatzoglou and Williams, 2016), and the accumulation of fuels due to effective fire suppression (Kreider et al.,  
2024), fire seasons have been increasing in duration, and are characterized by a greater number of large ( $\geq 200$  ha) and very  
large fires ( $> 100,000$  ha) (Government of Canada, 2026). Peatlands, which cover 25-30 % of the boreal forest region, and store  
over half of Canada's soil organic carbon (Government of Canada, 2026; Amiro et al., 2009), are particularly susceptible to  
25 fire in a warming climate. In 2023, Canada faced its most destructive wildfire season in history, with approximately 6,000 fires  
burning 18.5 million hectares, more than double the previous record set in 1989 (Government of Canada, 2024). This recent  
period of unprecedented fire activity in North America and worldwide is increasing the challenges associated with wildfires  
(Abatzoglou and Williams, 2016; Westerling et al., 2006).

In addition to emitting vast quantities of carbon dioxide ( $\text{CO}_2$ ), wildfires emit a variety of trace gas species including  
30 carbon monoxide (CO), methane ( $\text{CH}_4$ ), reactive nitrogen (Nr) species, and a wide spectrum of volatile organic compounds  
(VOCs) (Koss et al., 2018; Gilman et al., 2015; Burling et al., 2010; Yokelson et al., 2013; Akagi et al., 2011; Andreae, 2019;  
Watson et al., 2019). Nr, defined here as all nitrogen-containing compounds except  $\text{N}_2$  and  $\text{N}_2\text{O}$  (Roberts et al., 2020), includes  
both inorganic species such as nitrogen oxides ( $\text{NO}_x = \text{NO} + \text{NO}_2$ ), nitrous acid (HONO), and ammonia ( $\text{NH}_3$ ), as well as  
nitrogen-containing organic species, which are a subset of VOCs. Globally, wildfires release an estimated 400 teragrams of  
35 VOCs annually, making biomass burning the second-largest source of these compounds (Akagi et al., 2011). Once emitted,  
chemical transformations involving VOCs and Nr species within wildfire plumes result in the formation of secondary pollutants,  
including ozone and secondary particulate matter (Jaffe and Wigder, 2012; Alvarado and Prinn, 2009; Zhan et al., 2021).  
These wildfire pollutants can travel vast distances through the atmosphere, degrading air quality and introducing pollutants to  
downwind ecosystems, while also directly and indirectly impacting the earth's radiative balance (Miller et al., 2011; Rogers  
40 et al., 2020; Campos et al., 2019; Kallenborn et al., 2012; Sommers et al., 2014; Voulgarakis et al., 2015; Crutzen and Andreae,  
1990; Carter et al., 2019). In addition, many emitted VOCs are directly toxic (e.g., acrolein, acetaldehyde, hydrogen cyanide,  
acetonitrile, and benzene), making wildfire smoke a growing public health concern as evidence increasingly links exposure to  
adverse health effects (USEPA, 2019; Xiong et al., 2024). To mitigate against severe fire hazards, fuel reduction treatments,  
including vegetation thinning and prescribed burning, are increasingly being studied and employed (Agee and Skinner, 2005;  
45 Urbanski et al., 2022). A good understanding of the emission, transformation, and transport of VOC and reactive Nr species is  
essential to accurately modeling and evaluating the environmental and human health impacts of biomass burning, whether it  
be wildfires or prescribed burning.

Biomass burning emissions are typically estimated using bottom-up or hybrid approaches that combine activity data (e.g., fire  
radiative power (FRP), fuel consumption, area burned, fuel loading, fuel classification, combustion factor, etc.) with emission  
50 factors (i.e., EF, mass of emitted pollutant per mass of fuel consumed, on a dry fuel basis,  $\text{g kg}^{-1}$ ), emission ratios (i.e., ER,  
mass or molar ratio of emitted pollutant to another tracer, typically CO), or emission coefficients (i.e., mass of emitted pollutant  
per fire radiative energy,  $\text{g MJ}^{-1}$ ) (Chen et al., 2019; Copernicus Atmosphere Monitoring Service, 2022; Griffin et al., 2024;  
Wiedinmyer et al., 2023; Randerson et al., 2013). However, global and regional estimates of emissions from biomass burning



55 remain highly uncertain due to difficulties in accurately assessing activity data such as area burned and fuel consumption, and  
due to the high variability between individual fires (Carter et al., 2019; Pan et al., 2020; Jaffe et al., 2020). Another key source  
of uncertainty for models, and the focus of the current study, lies in the EFs themselves.

Wildfire models that use EF as critical inputs include: the Fire Inventory from NCAR (National Center for Atmospheric  
Research) (FINN) (Wiedinmyer et al., 2023), NASA's Global Fire Emissions Database (GFED) (Randerson et al., 2013),  
and the Canadian Forest Fire Emissions Prediction System (CFFEPS) developed by the Canadian Forest Service, which has  
60 recently been integrated into Environment and Climate Change Canada's (ECCC) FireWork (v2.0) air quality forecast model  
(Chen et al., 2019). Several wildfire emissions inventories have been compiled for this purpose and provide biomass burning  
EFs for a large number of gas and particle species, for various fuel or vegetation types (e.g., "Boreal forest", "Peat fires",  
etc.) (Akagi et al., 2011; Andreae, 2019; Binte Shahid et al., 2024; Urbanski, 2014; Andreae and Merlet, 2001). These EF are  
typically derived from field and laboratory studies.

65 Field studies (typically by aircraft) are invaluable for understanding real-world wildfire emissions and plume chemistry under  
natural fire conditions and for a representative fuel mix (Yokelson et al., 2008; Chen et al., 2010). However, limited observa-  
tional data, heterogeneity in fuel sources and combustion conditions, along with the coexistence of fresh and atmospherically-  
aged emissions, pose a challenge to deriving primary EFs for specific fuel types (Yokelson et al., 2013; Akagi et al., 2011;  
Andreae and Merlet, 2001). In contrast, controlled burning studies in the laboratory, and occasionally in the field, enable con-  
70 tinuous monitoring throughout all combustion phases with minimal interference. This approach allows key variables such as  
fuel type, fuel characteristics (e.g., moisture content and chemical composition), and fuel structure and arrangement to be con-  
trolled in a consistent and reproducible manner, yielding emissions data (e.g., EF, ER, and other observations of fire behavior)  
that are critical for interpreting complex real-world observations (Koss et al., 2018; Selimovic et al., 2019). Laboratory studies  
may also facilitate the deployment of a large suite of instruments in contrast to field studies, which often face greater challenges  
75 related to payload capacity. Recent advances in analytical instrumentation and techniques have further expanded the ability to  
quantify a wide range of emitted compounds (Burling et al., 2010; Yokelson et al., 2013, 1996; Stockwell et al., 2016).

During biomass burning, several processes occur, sometimes simultaneously, including a) distillation (which releases water  
vapour and other gases); b) pyrolysis of the biomass (e.g., cellulose, hemicellulose, and lignin) to produce flammable gases;  
c) flaming combustion; and d) smoldering/non-flaming processes such as glowing (Yokelson et al., 1996; Sekimoto et al.,  
80 2018). Fuel moisture content plays a significant role in governing the depth and extent of burning, and also influences the  
combustion efficiency, emission profile, and plume chemistry (Rein et al., 2008). Due to the complexity of the processes  
involved, both laboratory and field studies have demonstrated that pollutant EFs vary substantially depending on fuel type, fuel  
characteristics, and combustion conditions, reinforcing the need for studies specific to different vegetation/fuel types (Andreae,  
2019; Urbanski, 2014; Chen et al., 2010; Yokelson et al., 1996; Larkin et al., 2020; Kaiser et al., 2012; Cubison et al., 2011;  
85 Hecobian et al., 2011; Liu et al., 2017a).

The Canadian boreal region is dominated by peatlands, coniferous forests (e.g., black spruce, white spruce, jack pine, and  
balsam fir), with mixed-wood and deciduous stands (e.g., trembling aspen, white birch), and low-lying shrubs (Natural Re-  
sources Canada, 2025b; Forestry Canada, Fire Danger Group, 1992). These species contribute to a flammable layer of surface



fuels on the forest floor consisting of leaves, fine woody debris, bark, and needles that dry quickly (Patil Shirish et al., 2013).  
90 Below the surface litter is a slower-drying layer of decomposing organic materials that can support smoldering combustion.  
Additional Canadian surface fuels include grass, feather moss, and lichen, while deeper ground fuels include organic soils,  
duff, and peat (Urbanski et al., 2022). Surface and ground fuels account for more than 85 % of the total biomass consumed  
by Canadian forest fires, and the propensity of organic soil and peat to smolder over long durations makes them a key driver  
of wildfire emissions (Turetsky et al., 2015, 2011; Amiro et al., 2001; De Groot et al., 2009; Hu and Rein, 2022; Hu et al.,  
95 2018; Turetsky et al., 2002). In the future, boreal fires are expected to burn deeper and consume more fuel on a per-area basis  
(De Groot et al., 2009). Furthermore, human activities and droughts that lower the water table in peatlands are also expected  
to make these important carbon reservoirs more susceptible to fire (Hu et al., 2018; Rein, 2013). On the other hand, prescribed  
burning, often conducted during marginal conditions (higher atmospheric humidities and lower temperatures), targets the re-  
moval of rapidly burning light surface and understory fuels, including litter, fine woody debris, and grass, while avoiding  
100 canopy fuels or deeper ground fuels to reduce the likelihood of high-intensity fire when conditions are hotter and drier (Agee  
and Skinner, 2005; Urbanski et al., 2022).

Despite the regional and global importance of wildland (wildfire and prescribed burning) emissions from the Canadian boreal  
zone, fuel-specific EF data remain scarce for Canadian biomass fuels, particularly boreal surface and ground fuels such as peat,  
moss, and mulch. Only two aircraft campaigns (Hayden et al., 2022; Simpson et al., 2011) have measured comprehensive  
105 VOC emission from Canadian boreal wildfires, and few laboratory studies have systematically investigated the combustion of  
Canadian boreal fuels (Urbanski et al., 2022; Urbanski, 2014; Stockwell et al., 2015). The flaming and smoldering/residual  
combustion EF profiles used by CFFEPS to speciate emissions of non-methane organic compounds (NMOC) are based on  
the Urbanski (2014) EF inventories for “Wildfire Boreal Forest” and “Boreal Forest Duff/Organic Soil”, respectively (Chen  
et al., 2019; Simon et al., 2010). However, the “Wildfire Boreal Forest” dataset is based solely on the Simpson et al. (2011)  
110 aircraft study and a synthesis paper by Yokelson et al. (2013) that couples field and laboratory data, while the “Boreal Forest  
Duff/Organic Soil” dataset is based primarily on laboratory studies of duff/organic soil sourced from Montana and Northwest  
Territories (Bertschi et al., 2003) and a single laboratory burn of organic soil sourced from Alaska (Burling et al., 2010;  
Yokelson et al., 2013).

Addressing this gap, this study presents the first comprehensive analysis of VOCs and other trace gas emissions from labo-  
115 ratory burns of natural fuels relevant to Canadian wildfires, including boreal peat, black spruce forest mulch, grass, and other  
surface materials. EFs and ERs for volatile organic compounds and other trace gas species were derived, and their depen-  
dence on fuel type, fuel moisture content, and combustion behavior was investigated. The resulting dataset addresses key gaps  
in emission inventories, which will in turn improve emission representation for boreal fuels in wildland fire emission and  
chemical transport models.



## 120 2 Materials and methods

### 2.1 Fire lab experimental overview

The study was conducted in August, 2024 at the Fire Laboratory of Natural Resources Canada's Northern Forestry Centre in Edmonton, Alberta, Canada, as a part of the BBCan (Biomass Burning in Canada) campaign (Biomass Burning in Canada, 2021). An overview of the campaign and a schematic of the burning platform and instrumentation are provided in an overview paper (Moraes et al., 7 May 2026); the overall methodology is briefly described here. For each experiment, a fuel sample was placed on an aluminum tray and ignited using a quartz tube infrared electric heater (Model SIRH4002W, Stelpro Zenith), positioned about 5 cm above the fuel to initiate combustion, and then removed. Real-time fuel mass loss was monitored using a precision balance (Omega LSC7000-10), while air temperature was recorded using a fine wire thermocouple placed near the fuel surface at 1-second intervals throughout the entire burning period. Smoke generated during combustion was drawn into an overhead exhaust hood above the burn platform. A static mixer was installed in the exhaust duct to ensure uniform mixing of emissions, and airflow through the system was maintained using a regulated fan. Gas samples were collected from sampling ports located downstream of the static mixer and exhaust fan, ensuring representative capture of well-mixed combustion gases. To prevent particle interference with the gas analysis, Teflon filters (2.0  $\mu\text{m}$ ) were installed upstream of the analyzers and replaced daily. Additionally, all gas sampling lines were constructed from PFA and heated to 70° C to reduce losses of gaseous compounds due to condensation or surface adsorption.

### 2.2 Volatile organic compound measurements

In this study we quantified a total of 46 VOCs using an Iodide High Resolution Time-of-Flight Chemical Ionization Mass Spectrometer (I-CIMS) and Vocus Proton Transfer Reaction Time-of-Flight Mass Spectrometer (Vocus PTR-MS) (SI Table S1). These two measurement techniques provided complementary sensitivity to different chemical classes, together capturing a chemically diverse set of compounds representative of primary emissions from biomass combustion (as further discussed in SI Section S1 and illustrated in SI Fig. S1). Both instruments yield molecular formulae from high-resolution  $m/z$  detection. In the following, species are referred to by their molecular formula and also assigned to possible compounds based on a review of biomass burning studies, with details in SI Table S2. When comparing EFs to literature, reported EFs for all isomers for a given molecular formula are summed (e.g., for  $\text{C}_{10}\text{H}_{16}$ , the EF for all reported monoterpenes is summed). We acknowledge that differences between our study EFs and the literature EFs could be due to limitations in assigning  $m/z$  measured by the mass spectrometers to specific VOC isomers, application of calibration factors for a specific VOC isomer to the signal at a given  $m/z$ , or other interferences, such as from fragmentation (e.g., fragments contributing to  $\text{C}_5\text{H}_8$  - isoprene). The term total VOCs or  $\sum$  VOCs will be used to describe the sum of the 46 quantified VOCs. Low molecular weight compounds, such as methanol and formaldehyde, are not efficiently transmitted through the Vocus PTR-MS due to the influence of the big segmented quadrupole, while the selectivity of the ion chemistry limits the detection of small alkenes such as ethene and alkanes such as ethane and propane. These C1-C3 compounds are often found to contribute significantly to total biomass burning VOC emissions (Koss et al., 2018; Akagi et al., 2011; Urbanski, 2014; Hayden et al., 2022; Permar et al., 2021). In addition, common biomass burning



species such as methyl furan, acrylonitrile, methyl guaiacol, pyrrole, and pyridines were detected by Vocus PTR-MS but not quantified (Koss et al., 2018; Akagi et al., 2011; Sekimoto et al., 2018; Romanias et al., 2024).

## 155 2.2.1 I-CIMS

The I-CIMS was used to measure 22 volatile organic compounds (organic acids, isocyanic acid, and hydrogen cyanide), as well as nitrous acid (HONO) (Table S1). The I-CIMS (Aerodyne Research Inc.) used in this study is a modified version of a previously described instrument (Hayden et al., 2022; Young et al., 2024). The radioactive  $^{210}\text{Po}$  ion source has been replaced by a vacuum ultraviolet ionization source (VUV-IS) (Ji et al., 2020; Riva et al., 2024), and the ion-molecule reaction (IMR) region and inlet have been redesigned (Young et al., 2024). During BBCan, the IMR was operated at 50 mbar and 35° C. The I-CIMS sub-sampled (2450 sccm) perpendicular to a bypass line off the gas-phase inlet manifold (9.5 mm outer diameter PFA tubing) following dilution (2350 sccm of zero air). To minimize humidity effects, an additional 50 sccm flow of UHP  $\text{N}_2$  was directed through a room-temperature water bubbler and introduced directly to the IMR. The I-CIMS was operated at 1 Hz and had a mass resolution of  $\sim 5000 m/\Delta m$ .

165 Iodide reagent ions ( $\text{I}^-$ ) were generated by first passing a 250 sccm flow of UHP  $\text{N}_2$  over a permeation tube containing pure methyl iodide ( $\text{CH}_3\text{I}$ ) held at 40° C, then benzene ( $\text{C}_6\text{H}_6$ ) vapor was introduced to the  $\text{CH}_3\text{I}/\text{N}_2$  flow via a critical orifice above the headspace of a  $\text{C}_6\text{H}_6$  reservoir at 70° C before the  $\text{CH}_3\text{I}/\text{C}_6\text{H}_6/\text{N}_2$  flow passed through the VUV-IS and into the IMR.  $\text{C}_6\text{H}_6$  serves as a VUV absorber to produce additional photoelectrons that promote  $\text{I}^-$  generation (Ji et al., 2020).

Compounds were detected as iodide adducts ( $\text{I}\cdot\text{M}^-$ ) (Ji et al., 2020; Riva et al., 2024), and the mass spectra were analyzed using Tofware (v4.0.0). The ion signal ( $I_M$ , cps) for compound M was normalized to the sum of the reagent ion signals ( $\text{I}^-$  and  $\text{I}\cdot(\text{H}_2\text{O})^-$ ) and multiplied by  $10^6$  to yield the normalized ion signal ( $X_M$ , ncps) as follows in Equation (1).

$$X_M (\text{ncps}) = I_M (\text{cps}) \times \frac{10^6}{[I_I + I_{\text{I}\cdot\text{H}_2\text{O}}] (\text{cps})} \quad (1)$$

I-CIMS calibrations were performed before and after the campaign to determine sensitivities (ncps ppbv $^{-1}$ ) that were used to convert signal to mixing ratio; details of the calibration procedures are provided in SI Section S2.

## 175 2.2.2 Vocus PTR-MS

The Vocus PTR-MS (2R model, Aerodyne Research Inc.) was used to measure and quantify 24 VOCs (Table S1). The performance of this instrument model has been described elsewhere (Krechmer et al., 2018; Link et al., 2025). The drift tube was operated at 2.2 mbar and 60° C. The axial voltages were 600 V (entry) and 20 V (exit), with the 450 V quadrupole amplitude voltage applied at a frequency of 1.3 MHz for a resulting E/N (reduced electric field) of  $\sim 120$  Td. During BBCan, the Vocus PTR-MS made 1 Hz measurements and had a mass resolution of  $\sim 7000 m/\Delta m$ .

A bypass pump sub-sampled  $\sim 2500$  sccm from the gas-phase inlet manifold (9.5 mm PFA tubing). The Vocus PTR-MS sub-sampled ( $\sim 100$  sccm) perpendicular to the bypass flow through a short piece of PEEK tubing. The vapour from a permeation



185 tube containing trichlorobenzene at room temperature was passively introduced to the bypass flow as a mass calibrant ( $m/z$  182). Compounds were detected and quantified as protonated formulae (i.e.,  $MH^+$ ) (De Gouw and Warneke, 2007), and mass spectra were analyzed using Tofware (v4.0.0). Unique peak lists were created for each fuel type, and sensitivities in cps  $ppbv^{-1}$  were applied to convert ion signals (cps) to mixing ratio (ppbv). Multi-point calibrations using a custom standard cylinder (Ionicon) were performed daily during the campaign, and additional calibrations were performed before and after the campaign (see SI section S2 for further details).

### 2.3 Additional measurements

190 Several other gas-phase and particle-phase species were measured during the BBCan laboratory campaign, with instrumentation as described in the overview paper (Moraes et al., 7 May 2026). CO, CO<sub>2</sub>, and CH<sub>4</sub> were quantified using cavity ring-down spectroscopy (Picarro G2401-m gas analyzer). A second Picarro G2401-m analyzer measured total gaseous carbon (TC, in units of ppm C) after passing sample air through a catalyst to convert all gaseous carbon-containing species to CO<sub>2</sub> (Hayden et al., 2022). Total non-methane organic compound (NMOC) in units of ppm C was calculated by subtracting the CO, CO<sub>2</sub>, and CH<sub>4</sub> 195 measured by the first Picarro (i.e., instrument without the catalyst) from the TC measurements. In the manuscript, the term NMOC describes emissions in carbon units (i.e., NMOC EF in g C kg<sup>-1</sup>). To distinguish NMOC emissions in mass units (directly reported by other studies, or after converting NMOC from carbon to mass units), the term NMOC<sub>G</sub> (i.e., NMOC<sub>G</sub> EF in g kg<sup>-1</sup>) is used. Nitrogen oxides (NO and NO<sub>2</sub>) were measured separately using a Cavity Attenuated Phase Shift NO<sub>X</sub> analyzer (N500, Teledyne API) (Teledyne, 2025) and ammonia (NH<sub>3</sub>) was measured using an H<sub>2</sub>S/NH<sub>3</sub> analyzer (911-0039, 200 ABB-LGR) (Los Gatos Research, 2025). EFs for CO, CO<sub>2</sub>, CH<sub>4</sub>, TC, NH<sub>3</sub>, NO, and NO<sub>2</sub> are reported by Hanashiro Moraes et al. (2026).

### 2.4 Biomass fuel samples

205 Six biomass fuel types were burned during the BBCan campaign: two peat fuels (PF, PM), mulch (MU), grass (GR), ponderosa pine needles (PN), and “surface material” (SM), which was composed of dead leaves, needles, and small branches (Moraes et al., 7 May 2026). Peat fuels included two subtypes: compacted peat with surface mulch (PM) and peat with surface moss (PF), with dimensions of roughly 254 x 508 x 508 mm. All peat and mulch samples were collected from the Pelican Mountain Research Site in Alberta, Canada, which is a bog and fen-type ecosystem dominated by black spruce (*Picea mariana*) (Thompson et al., 2020; Moore et al., 2020). Peat with moss was collected from the natural forest floor to represent peat with minimal anthropogenic disturbance, while peat with mulch was collected from the floor of open areas to represent areas that 210 have been harvested or treated by humans. GR (*Elymus trachycaulus* and *Bromus inermis*) and SM were collected near Edmonton, Alberta and include species common to the Canadian Prairies. Ponderosa pine needles were sourced from Kamloops, British Columbia. PN is not considered a boreal fuel, but was included due to its abundance in Western North America and its well-documented combustion and emission characteristics, making it a valuable reference biomass (Burling et al., 2010; Chen et al., 2007).



215 Moisture content and elemental composition of the studied fuel types were determined according to methods described in  
Section S3 and are listed in Table 1, along with their assignment to Canadian Forest Fire Behavior Prediction System (FBP) fuel  
types, which are used in CFFEPS (Chen et al., 2019; Natural Resources Canada, 2025b). The experiments focused primarily  
on samples that had been subjected to drying prior to combustion; such samples are labelled as “dry” and include all fuel types  
with the exception of PN. PN is labelled as “wet” since it was not dried prior to burning, but its natural moisture content was  
220 relatively low ( $\sim 13\%$ ), similar to the dry samples, and so it is included in discussions with the dried, “low moisture-content”  
fuels. To study the influence of moisture content on emissions, experiments were also performed on a subset of samples (PM,  
PF, MU) left in their natural state, and these samples are labelled as “wet”. MU (wet) also had a low moisture content ( $\sim 7\%$ ),  
but it is considered with the wet fuels because it can be contrasted to the dried sample, MU (dry) ( $\sim 4\%$ ). The PF (wet) samples  
had high moisture content (top 5 cm  $\sim 30\%$ , bottom 5 cm  $\sim 110\%$ , overall  $\sim 51\%$ ), which resulted in a short smoldering  
225 period with a large amount of unburnt fuel, and only one sample was burnt. The PM (wet) samples (top 5 cm  $\sim 50\%$ , bottom 5  
cm  $> 200\%$ , overall  $\sim 100\%$ ) did not sustain combustion beyond a short flaming period. Although the high moisture content  
of natural peat fuels provides resistance to combustion, smoldering of peat fuels can occur in high-intensity wildfires when  
heat from the combustion of surrounding fuels facilitates drying in advance of the wildfire front (Watson et al., 2019; Hu et al.,  
2018). Furthermore, under experimental fires with high-intensity fire conditions, despite patches of high peat surface moisture,  
230 the upper 1-2 cm of moss and/or peat fuel is observed as being combusted during the main fire front passage without further  
self-sustaining smoldering (Wilkinson et al., 2018). This externally driven peat combustion is due to the large, directed heat  
pulse from the large flaming front to the peat surface (Thompson et al., 2015).

## 2.5 Emission factors, emission ratios, and modified combustion efficiency

EF and ER were derived for quantified VOCs and other trace gases. EF, expressed in g emitted per kg of dry fuel consumption  
235 were calculated following the methodology described by Hanashiro Moraes et al. (2026) (Andreae, 2019; Hu et al., 2019).

Briefly, the EF for species X ( $EF_X$ ) was calculated following Equation (2):

$$EF_X (g kg^{-1}) = \frac{\int_{t_i}^{t_f} \Delta X(t) \times 10^9 \times \frac{MW_X}{V_{air}} \times Q_{duct}(t) dt}{TFC} \quad (2)$$

where  $\Delta X(t)$  (ppb) is the background-corrected mixing ratio of species X at time t,  $MW_X$  ( $g mol^{-1}$ ) is the molecular  
weight of species X,  $V_{air}$  ( $m^3 mol^{-1}$ ) is the molar volume of air at standard temperature and pressure,  $Q_{duct}(t)$  ( $m^3 s^{-1}$ )  
240 is the volumetric flow rate of the duct at time t, and TFC (kg, dry fuel) is the total fuel consumption. TFC was calculated  
from real-time weight measurements for each burn, corrected for moisture content (Moraes et al., 7 May 2026). The integral is  
calculated from ignition (initial t,  $t_i$ ) to extinction (final t,  $t_f$ ) for overall (i.e., entire burn) EFs.



The ER of a pollutant is also commonly expressed relative to a co-emitted, relatively inert species such as CO or CO<sub>2</sub> (Akagi et al., 2011; Andreae, 2019). When direct fuel consumption measurements are not feasible, EF (g kg<sup>-1</sup>) can be derived from ER using the carbon mass balance approach (Koss et al., 2018; Akagi et al., 2011; Andreae, 2019; Selimovic et al., 2018; Ward and Radke, 1993). The choice of reference gas is critical, as CO<sub>2</sub> predominantly reflects efficient flaming combustion, while CO is characteristic of incomplete, smoldering combustion (Gilman et al., 2015). CO is typically selected due to its long atmospheric lifetime (1–4 months) (Hayden et al., 2022; Seinfeld and Pandis, 2016) and its strong correlation with a wide range of emitted gases (Koss et al., 2018; Gilman et al., 2015; Liu et al., 2017b; Koppmann et al., 2005).

Accordingly, the ER<sub>X</sub> for species X was determined using Equation (3):

$$ER_X \text{ (ppbv/ppmv)} = \frac{EF_X}{EF_{CO}} \times \frac{MW_{CO}}{MW_X} \times 1000 \quad (3)$$

where EF<sub>CO</sub> and MW<sub>CO</sub> are the EF and molecular weights of CO, respectively. The ERs are provided (Table S3) to facilitate comparison with prior studies and so that they may be incorporated into atmospheric models. However, the discussion below focuses only on the derived EFs.

Biomass burning emissions vary significantly between combustion processes such as flaming and smoldering (Gilman et al., 2015; Selimovic et al., 2019; Majluf et al., 2022). Modified combustion efficiency (MCE) is often used to describe the relative contributions of flaming and smoldering combustion, as defined by Equation (4) (Yokelson et al., 2013; Akagi et al., 2011; Yokelson et al., 1996; Hu et al., 2019; Ward and Radke, 1993):

$$MCE = \frac{\Delta CO_2}{\Delta CO_2 + \Delta CO} \quad (4)$$

where ΔCO<sub>2</sub> and ΔCO denote the background-corrected mixing ratios of CO<sub>2</sub> and CO, respectively. MCE values ~ 0.99 are representative of pure flaming combustion while MCE ~ 0.80 are representative of pure smoldering combustion (Akagi et al., 2011; Urbanski et al., 2022; Yokelson et al., 1997). To assess the variability of emissions across combustion phases, EF and ER were determined separately for the flaming and smoldering phases using MCE to determine the transition time (t<sub>t</sub>). In this study, MCE values ≥ 0.90 were designated as indicative of flaming combustion, and t<sub>t</sub> was defined as the time when the instantaneous MCE first dropped below 0.90 and then remained below that threshold for at least 3 consecutive minutes (Akagi et al., 2011; Liu et al., 2017b). The flaming-phase and smoldering-phase EF were calculated using Equation (2), substituting the appropriate bounds of integration (i.e., t<sub>i</sub> to t<sub>t</sub> for flaming, and t<sub>t</sub> to t<sub>f</sub> for smoldering). Similarly, overall (commonly referred to as fire-integrated) as well as combustion-phase resolved MCE were calculated by integrating Equation (4) over the appropriate bounds of integration.

While we did not perform wall-loss and partitioning delay analysis, it is worth noting that they may influence the observed time series and bias phase-resolved EF estimates (De Gouw and Warneke, 2007; Pagonis et al., 2017). For instance, “sticky” VOCs emitted predominantly during flaming may exhibit partitioning delays, leading to an apparent reduction in flaming-



phase EFs and a corresponding enhancement of smoldering-phase EFs. These effects are unlikely to alter overall EF, but we acknowledge they may influence the relative magnitude of phase-resolved EFs for a small number of VOCs in this study (e.g.,  
275  $C_7H_8O_2$ ).

EFs and ERs in the tables and text are presented as mean values  $\pm$  standard deviation. The largest sources of uncertainty are the variance between tests (on average the relative standard deviation is  $> 50\%$ ), the uncertainty in the flow rate in the exhaust duct ( $\pm 12.2\%$ ) (Moraes et al., 7 May 2026), and the uncertainty in the sensitivities used to convert signal to mixing ratio, which are estimated to range from 20-30% depending on the species and the calibration method.

## 280 3 Results and discussion

### 3.1 Temporal emission profiles

Fig. 1 illustrates high-resolution (1 s) temporal profiles of key combustion parameters (fuel mass, air temperature at the fuel surface, and MCE) and background-subtracted mixing ratios of  $CO$ ,  $CO_2$ , and selected VOC ( $CH_2O_2$ ,  $C_5H_4O_2$ ,  $C_2H_4O_2$ , and HCN) for a representative laboratory burn of PF (dry). Upon ignition, the fuel burns by flaming combustion and the mixing  
285 ratios of  $CO_2$  and  $CO$  (panel 1b) increase sharply along with temperature, indicative of high-temperature pyrolysis. The MCE during this period of flaming combustion (panel 1a, yellow shaded area) reaches a mean of 0.90, reflecting efficient oxidation. After a short flaming phase, the  $CO_2$  and  $CO$  mixing ratios decrease rapidly, the MCE drops below 0.90, and the fire transitions into a prolonged smoldering phase. The smoldering phase is characterized by broader, delayed emission of  $CO$  and other incomplete combustion products (e.g., such as the VOC displayed in panel 1c) and lower temperatures (i.e., low-temperature  
290 pyrolysis), with temporal profiles similar to those observed in biomass burning studies (Burling et al., 2010; Akagi et al., 2011; Andreae, 2019; Stockwell et al., 2016). The MCE decreases accordingly, to a final fire-integrated value of 0.75. The fuel mass (panel 1a) decreases rapidly during the flaming stage and more slowly during the low-temperature smoldering phase. As the fuel is consumed and the combustion progresses towards extinction, mixing ratios (i.e., emissions) of  $CO$  and VOC decrease, temperature decreases, fuel consumption slows, and the MCE values become increasingly erratic due to low mixing ratios of  
295  $CO_2$  and  $CO$ . As illustrated by panel 1c, the VOC temporal profiles are generally correlated with the  $CO$  temporal profile, supporting the use of ERs (Gilman et al., 2015; Majluf et al., 2022).

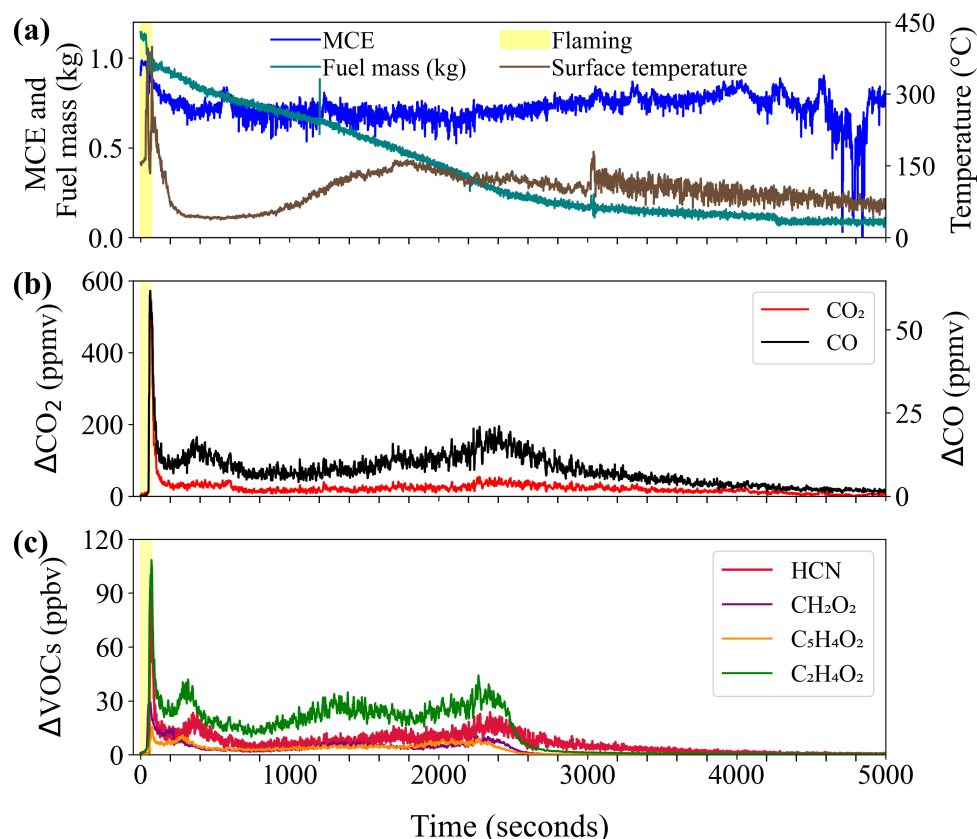


**Figure 1.** Temporal emission profiles from a representative laboratory burn of PF (dry): (a) MCE (blue), fuel mass in kg (teal), and air temperature at the fuel surface in °C (brown); the flaming phase is indicated by the shaded (yellow) region, and the subsequent smoldering phase is colorless. (b) Background-subtracted mixing ratios (ppmv) of CO<sub>2</sub> (red) and CO (black). (c) Background-subtracted mixing ratios of VOCs (ppbv), including HCN (crimson), CH<sub>2</sub>O<sub>2</sub> (purple), C<sub>5</sub>H<sub>4</sub>O<sub>2</sub> (orange), and C<sub>2</sub>H<sub>4</sub>O<sub>2</sub> (green) measured by Vocus PTR-MS and I-CIMS.

### 3.2 Overview of trace gas emission factors

Mean overall EFs ( $\text{g kg}^{-1}$ ) ( $\pm$  standard deviation) for the 46 quantified VOCs and HONO are listed for each biomass type in Table 1, along with mean NMOC EF and  $\sum$  VOCs EF. The mean flaming-phase and smoldering-phase EFs are provided in Table S2. The mean overall and combustion-phase resolved ERs (ppbv VOC/ppmv CO) are listed in Table S3. The quantified VOC species cover several important compound classes, including oxygenates, furanoids, phenolic compounds, terpenoids, aromatics, and nitrogen-containing species, which are consistently reported among the dominant contributors to wildfire VOC emissions (Hayden et al., 2022; Simpson et al., 2011). Fig. 2 presents mean overall EF ( $\text{g kg}^{-1}$ ) for a subset of 22 VOCs along with HONO for the studied biomass types and moisture conditions (colored points), together with reported ranges (orange bars) from literature sources, which include emission inventories for “Peatlands” (Binte Shahid et al., 2024) and “Boreal Forest” (Akagi et al., 2011; Andreae, 2019; Binte Shahid et al., 2024; Urbanski, 2014), aircraft measurements (Hayden et al., 2022; Simpson et al., 2011; Permar et al., 2021), and a recent laboratory study (Koss et al., 2018).



As demonstrated by Fig. 2 and Fig. S2, the VOC emission magnitudes and emission profile (relative emissions) vary considerably by fuel type and moisture content. We find that CHO compounds dominate emissions across all fuel types, with contributions to the  $\sum$  VOCs EF ranging from 46 % to 78 %, consistent with the high contributions of CHO reported in the literature (Koss et al., 2016; Gilman et al., 2015; Permar et al., 2021), and also due to the high selectivity of the Vocus PTR-MS and I-CIMS to oxygenates. CHO compounds such as  $\text{CH}_2\text{O}_2$  (formic acid),  $\text{C}_2\text{H}_4\text{O}_2$  (acetic acid, with smaller contributions from glycolaldehyde),  $\text{C}_5\text{H}_4\text{O}_2$  (furfural), and  $\text{C}_4\text{H}_4\text{O}$  (furan) consistently rank among the most abundant species for all studied fuel types, underscoring their widespread presence in biomass burning emissions.  $\text{C}_2\text{H}_4\text{O}_2$  (acetic acid, glycolaldehyde) is the largest contributor to the  $\sum$  VOCs EF for the dry peat fuels and SM (dry), with the highest EF for PF (dry) at  $4.75 \pm 0.45 \text{ g kg}^{-1}$ , followed by PM (dry) ( $2.95 \pm 1.75 \text{ g kg}^{-1}$ ).  $\text{CH}_2\text{O}_2$  (formic acid) is the largest contributor to  $\sum$  VOCs EF for MU (dry and wet) and also ranks above  $\text{C}_2\text{H}_4\text{O}_2$  (acetic acid) for PN (wet) and PM (wet). The highest  $\text{CH}_2\text{O}_2$  (formic acid) EF across all biomass types and moisture conditions is observed for PM (wet) ( $2.56 \pm 1.78 \text{ g kg}^{-1}$ ). The wet peat fuels also have higher relative contributions from  $\text{C}_3\text{H}_4\text{O}_3$  (pyruvic acid) and  $\text{C}_2\text{H}_4\text{O}$  (acrylic acid) compared to their dry counterparts. Other dominant oxygenates across fuels include  $\text{C}_2\text{H}_4\text{O}$  (acetaldehyde),  $\text{C}_3\text{H}_6\text{O}$  (acetone, with possible contributions from propanal), and phenolic compounds such as  $\text{C}_6\text{H}_6\text{O}_2$  (methylfurfural, benzenediols such as catechol and resorcinol) and  $\text{C}_7\text{H}_8\text{O}_2$  (guaiacol and isomers). PN and SM emit a greater proportion of CH compounds (35 % and 22 % of  $\sum$  VOCs EF, respectively) compared to other fuel types, with high contributions from aromatics,  $\text{C}_{10}\text{H}_8$  (naphthalene), and  $\text{C}_8\text{H}_8$  (styrene).  $\text{C}_{10}\text{H}_{16}$  (monoterpene) EFs are highest for PN (wet) ( $0.38 \pm 0.09 \text{ g kg}^{-1}$ ), SM (dry) ( $0.27 \pm 0.02 \text{ g kg}^{-1}$ ), and PF (dry) ( $0.14 \pm 0.06 \text{ g kg}^{-1}$ ), and  $< 0.1 \text{ g kg}^{-1}$  for all other fuels. The relative contribution of  $\text{C}_6\text{H}_6$  (benzene),  $\text{C}_8\text{H}_8$  (styrene), and  $\text{C}_{10}\text{H}_8$  (naphthalene) to  $\sum$  VOCs EF is also enhanced for the wet peat fuels. With respect to nitrogen-containing VOC, we observe significant emissions of HCN (hydrogen cyanide) and  $\text{C}_2\text{H}_3\text{N}$  (acetonitrile) across all fuels, although the CHN class is most prominent for the wet and dry peat fuels, with PM (wet) showing the highest CHN contribution (21 % of  $\sum$  VOCs EF). Emissions of Nr are discussed in greater detail in Section 3.5.

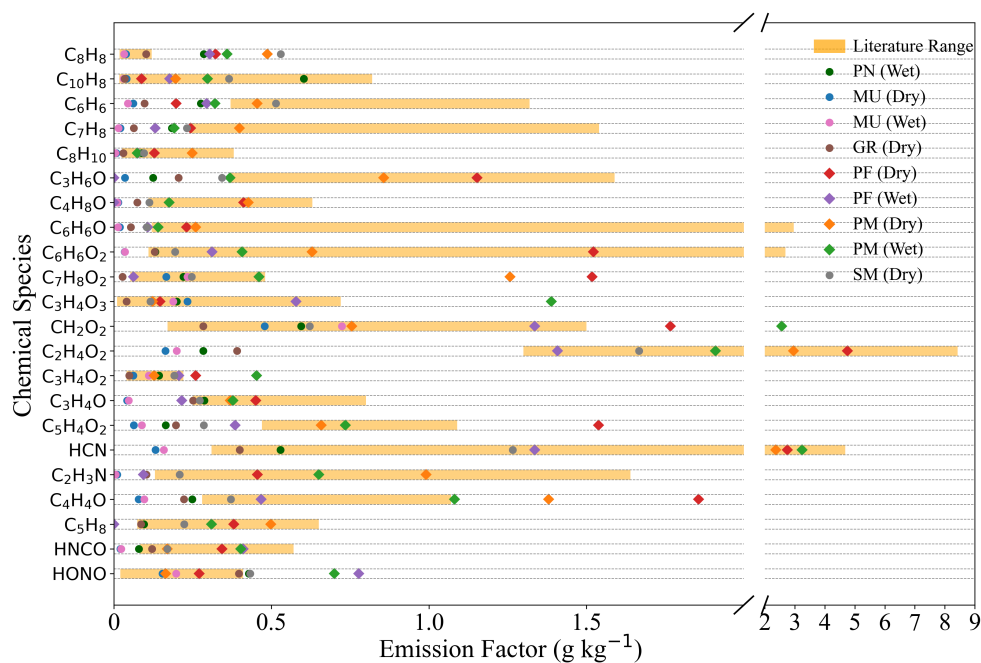


**Figure 2.** Mean EF ( $\text{g kg}^{-1}$ ) of individual VOCs from biomass fuel types (PN, MU, GR, PF, PM, and SM, under wet and dry conditions; colored symbols) compared to literature EF ranges (orange bars). Literature used for the comparison include laboratory, field studies and emission inventories for Boreal Forests and Peatlands (Koss et al., 2018; Akagi et al., 2011; Andreae, 2019; Binte Shahid et al., 2024; Urbanski, 2014; Hayden et al., 2022; Simpson et al., 2011; Permar et al., 2021), as listed in (SI Table S4). The peat fuels (PM, PF) are represented as diamonds for emphasis, and the remaining fuels are represented as circles.

330 The mean EFs from this study generally fall within reported ranges. However, as illustrated by Fig. 2, there are several VOC  
 for which measured EF fall below the literature range, particularly for non-peat fuels. On the other hand, VOC EF for peat  
 fuels (PF, PM) are at the high end, and in some cases exceeding the literature range for several VOC, including  $\text{CH}_2\text{O}_2$  (formic  
 acid),  $\text{C}_4\text{H}_4\text{O}$  (furan),  $\text{C}_5\text{H}_4\text{O}_2$  (furfural), and  $\text{C}_7\text{H}_8\text{O}_2$  (guaiacol and isomers). High emissions of guaiacol are associated with  
 smoldering, and it should be noted that the literature EF for guaiacol are limited to three studies (Koss et al., 2018; Hayden  
 335 et al., 2022; Permar et al., 2021) in Fig. 2, none of which are laboratory studies of peat or organic soil combustion. High EF for  
 peat fuels are consistent with their low MCE, as described below. Another exception is styrene ( $\text{C}_8\text{H}_8$ ), for which we observe  
 systematically higher EF than reported for all fuels except MU and GR.

### 3.3 Total non-methane organic compound (NMOC) emissions

Figs. 3a and 3b show the contribution of  $\text{CO}_2$ ,  $\text{CO}$ ,  $\text{CH}_4$ , and NMOC to the total gaseous carbon (TC) emissions for each  
 340 fuel type in absolute terms ( $\text{g C kg}^{-1}$ ) and as percentage contributions, respectively. The mean fire-integrated MCE values  
 are shown for each biomass type in Fig. 3c, with the low moisture-content fuels displayed on the left (brown), and the ‘wet’  
 PM, PF, and MU fuels on the right (yellow). Fig. 3d shows the contribution of the total quantified VOCs ( $\sum \text{VOCs}$ ; solid  
 brown and yellow; also expressed in  $\text{g of C kg}^{-1}$  of fuel) to the total measured NMOC EF for each fuel type, with the percent



contribution of  $\sum$  VOCs to NMOC displayed at the top of each bar. The quantified  $\sum$  VOCs constituted 13–34 % of total  
 345 NMOC on a carbon basis, with the highest contribution for the peat fuels (PM and PF) and PN, and the lowest for GR and  
 MU. A significant missing NMOC fraction is expected, given the limited number of species quantified by the Vocus PTR-MS  
 and I-CIMS (Section 2.2). The missing NMOC likely also includes a large fraction of intermediate volatility or semivolatile  
 compounds (I/SVOC). Previous studies suggest this fraction may contribute from > 5 % to almost 40 % depending on the fuel  
 type, and the definition of I/SVOC (Yokelson et al., 2013; Hayden et al., 2022; Hatch et al., 2018).

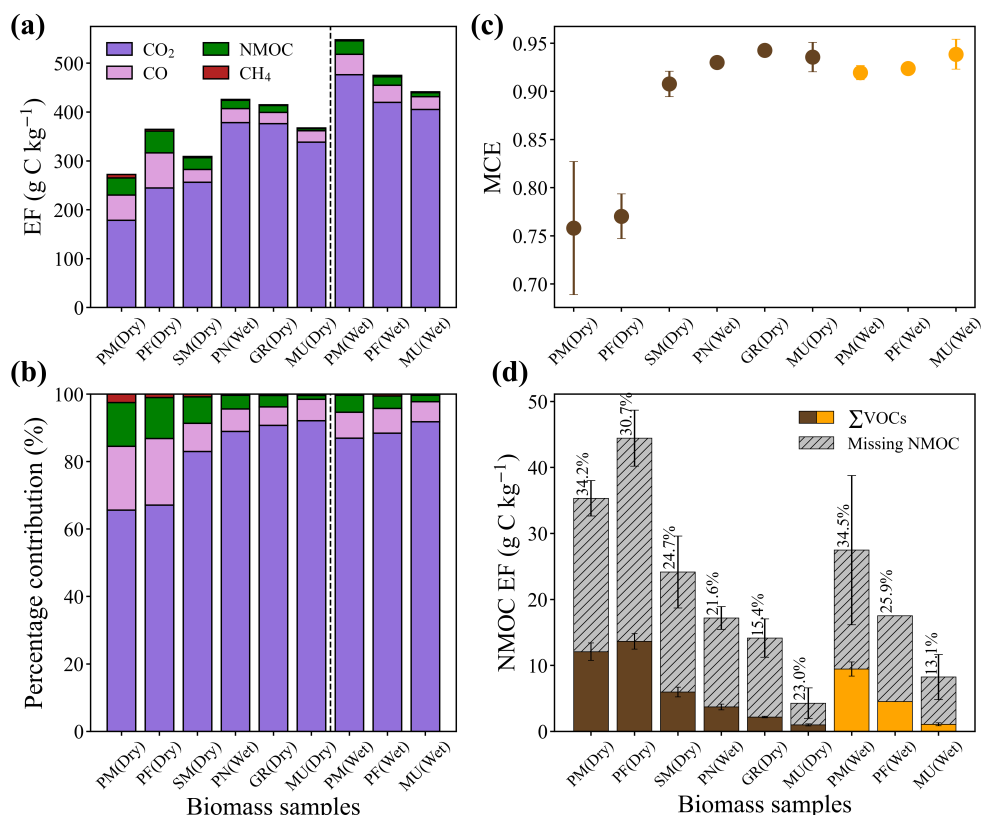


**Figure 3.** (a) Mean overall EF for CO<sub>2</sub> (purple), CO (pink), CH<sub>4</sub> (red), and NMOC (green) expressed in carbon units (g C kg<sup>-1</sup>); (b) their percentage contributions to TC (g C kg<sup>-1</sup>) for each biomass type; (c) mean fire-integrated MCE for each biomass type; and (d) mean overall NMOC EF (g C kg<sup>-1</sup>) for each biomass type, with mean overall  $\sum$  VOCs (solid brown and yellow, sum of quantified VOC) and missing NMOC (grey stripes). The percentage values indicate the contribution of  $\sum$  VOCs EF to the total NMOC EF. Error bars in (c) and (d) indicate the standard deviation of the mean. In (c) and (d), brown is used for low-moisture content fuels and yellow is used for wet fuels.

350 Fig. 3a and 3b demonstrate that gas-phase carbon is emitted primarily as CO<sub>2</sub> across all species (66–92 %), with smaller  
 contributions from CO (6–20 %), NMOC (1–13 %), and CH<sub>4</sub> (< 1 %), with the absolute magnitude and distribution of emissions  
 varying depending on the biomass type. Note that emission factors for particulate organic carbon and elemental carbon from  
 offline analysis of filter samples are presented in the overview paper (Moraes et al., 7 May 2026). Among the biomass types,  
 the dry peat fuels (PF and PM) are prone to extensive smoldering (Turetsky et al., 2011, 2015), and burn with characteristically



355 low combustion efficiency (fire-integrated MCE, 0.76-0.77) as shown in Fig. 2c. The low MCE values observed in this study  
are at the low end of the range observed by other laboratory studies of peat fuels (0.77-0.90) (Watson et al., 2019), including  
Canadian peat (MCE = 0.81) (Stockwell et al., 2014). Accordingly, the dry peat fuels exhibit the highest NMOC EF due to  
a greater contribution from incomplete combustion products compared to the other fuels, with NMOC accounting for about  
12-13 % of the TC. In contrast, MU (dry and wet) and GR (dry) burn very efficiently via flaming combustion (fire-integrated  
360 MCE  $\sim$  0.95), while PN (wet) and SM (dry) display intermediate MCE values ( $\sim$  0.93 and  $\sim$  0.91, respectively). In fact, GR  
(dry) combusted entirely during the flaming stage with no identifiable smoldering phase based on MCE.

### 3.4 Dependence of EF on MCE

#### NMOC and $\sum$ VOCs

Several studies have demonstrated that for many compounds, EF is anti-correlated with MCE, and that these relationships can  
365 be helpful for extrapolating EF to real-world MCE and for comparing EF across fuel types (Yokelson et al., 2013; Urbanski  
et al., 2022; Permar et al., 2021; Selimovic et al., 2018; Stockwell et al., 2014). The mean overall (circles), flaming-phase  
(squares), and smoldering-phase (triangles) NMOC EFs are plotted as a function of their respective mean integrated MCEs for  
all fuel types in Fig. 4, along with a linear fit to the low moisture-content data. An inverse linear relationship is evident ( $R^2$   
= 0.59), illustrating that the overall variation in NMOC emissions within and between fuels is largely driven by combustion  
370 efficiency (i.e., degree of smoldering vs. flaming combustion). The same trend is also evident when considering all individual  
burn data (SI Fig. S3), reinforcing that the observed relationships are robust and not an artifact of averaging.

Interestingly, the dry and wet MU samples exhibit unique behavior and show a very weak relationship with MCE compared  
to the other fuels. Lower emissions from PM (peat with mulch) compared to PF (peat with moss) are consistent with the low  
NMOC EF for mulch on its own. Interestingly, the human-influenced peat (PM) has higher methane EFs (Moraes et al., 7 May  
375 2026), but lower NMOC and CO EFs than the natural peat (PF). PF (wet) and PM (wet) extinguished shortly after smoldering  
began, leaving a substantial fraction of unburnt fuel (98–99 %), highlighting the inhibitory effect of high moisture content  
on sustained smoldering combustion. Their respective NMOC EFs are consistent with the high MCE associated with flaming  
combustion.

The same plot as Fig. 4 but for total  $\sum$  VOCs EF ( $\text{g kg}^{-1}$ ) is provided in SI Fig. S4. Similar trends are evident for  $\sum$  VOCs  
380 EF, although the relationship with MCE is weaker, particularly for PN (wet) and SM (dry). This may indicate that a substantial  
fraction of the additional emissions during smoldering is associated with unquantified compounds that are not fully captured  
within the  $\sum$  VOCs. The weaker relationship between  $\sum$  VOCs and MCE, together with the variation in the contribution of  
 $\sum$  VOCs to NMOC across fuel types (Fig. 3d) indicates that the VOC speciation profile and individual VOC EFs are dependent  
on other factors as well.

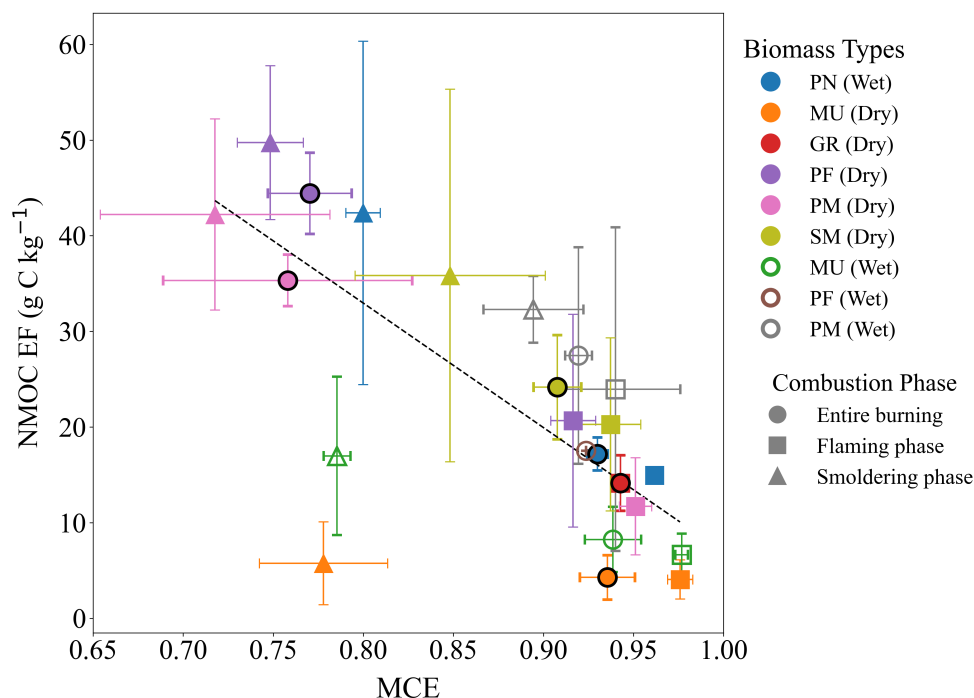


**Figure 4.** NMOC EF ( $\text{g C kg}^{-1}$ ) as a function of MCE across various biomass fuel types. Data are shown for the entire burning period (circles), flaming phase (squares), and smoldering phase (triangles). Vertical and horizontal error bars represent the standard deviation of the mean NMOC and MCE, respectively. The dashed line is the linear regression to data points for low-moisture content fuels (solid symbols), with slope (-130), intercept (137.06), and  $R^2$  (0.59). Entire burn data are highlighted with a bold black outline, while open symbols denote MU (wet), PM (wet), and PF (wet) fuels.

### 385 Individual VOC

Fig. 5 illustrates the relationship between overall EFs ( $\text{g kg}^{-1}$ ) and fire-integrated MCE for four example VOCs: (a)  $\text{CH}_2\text{O}_2$  (formic acid), (b) HCN (hydrogen cyanide) (c)  $\text{C}_6\text{H}_6$  (benzene) and (d)  $\text{C}_4\text{H}_4\text{O}$  (furan). The low-moisture content fuels (teal squares) are distinguished from the ‘wet’ fuels (blue diamonds). Similar relationships for  $\text{CH}_4$  (methane) and an additional 19 VOC are displayed in SI Fig. S5.

390 As with NMOC, the individual VOC EFs derived from this study (teal squares in Fig. 5 and Fig. S5) are inversely proportional to MCE for  $\text{CH}_4$  (Fig. S5a) and most of the quantified VOCs. However, for several VOCs, the relationship is weaker or less clear, and in some cases, similar or lower EFs are observed for smoldering fuels (i.e., peat fuels) compared to flaming fuels (i.e., GR and MU), despite much lower MCE. For example, this behavior is observed for many CH compounds such as  $\text{C}_6\text{H}_6$  (benzene) (Fig. 5c),  $\text{C}_8\text{H}_8$  (styrene, Fig. S5m),  $\text{C}_{10}\text{H}_8$  (naphthalene, Fig. S5r), and  $\text{C}_{10}\text{H}_{16}$  (monoterpenes, Fig. S5t), as well  
 395 as some non-CH compounds such as  $\text{C}_3\text{H}_4\text{O}_3$  (pyruvic acid, Fig. S5h). The plots in Fig. 5 and Fig. S5 also display literature EF from select wildfire studies (Hayden et al., 2022; Simpson et al., 2011; Permar et al., 2021), laboratory burns (Koss et al., 2018; Yokelson et al., 2013; Stockwell et al., 2015; Bertschi et al., 2003; Selimovic et al., 2018), and EF compilations (Akagi et al., 2011; Andreae, 2019; Binte Shahid et al., 2024; Urbanski, 2014), with additional details in SI Section S5. The literature



EF vs MCE relationships in these figures provide additional context for interpreting the literature comparisons presented above  
400 (Section 3.2) (i.e., for many VOC, high EF for peat fuels are consistent with their low MCE). However, together with the EFs  
from this study, the additional literature values demonstrate that the relationship between EF and MCE is well constrained and  
relatively independent of fuel type and/or study type for some VOC (e.g., CH<sub>4</sub>, HCN, C<sub>4</sub>H<sub>4</sub>O) and poorly for others. This  
indicates that additional factors likely play an important role in determining VOC emissions (Andreae, 2019; Permar et al.,  
2021).

405 In particular, VOC emissions are associated with the pyrolysis of biopolymers (i.e., cellulose, hemicellulose, and lignin),  
with the pyrolysis temperature playing an important role in determining the functionality of emitted species (Sekimoto et al.,  
2018; Romanias et al., 2024). Aromatization (leading to aromatics such as naphthalene, benzene, and phenol) is a result of  
high-temperature pyrolysis, whereas depolymerization (leading to furanoids and phenolic compounds such as guaiacol) is a  
result of low-temperature pyrolysis. As such, Sekimoto et al. (2018) found that high- and low-temperature pyrolysis profiles  
410 could adequately describe VOC emissions from controlled laboratory burns of a wide variety of fuels during FIREX 2016.  
While a transition from high to low MCE may reflect a transition from high- to low-temperature pyrolysis, the correspondence  
may not be exact, and as a result, MCE may not be the most useful predictor for certain VOC EFs. It is further expected that  
the biopolymer content of the fuels, which impacts the pyrolysis pathways (Romanias et al., 2024; Hatch et al., 2018), will  
also play a role in determining the speciation of emitted VOC. Indeed, higher EF for phenolic species (C<sub>6</sub>H<sub>6</sub>O<sub>2</sub>, C<sub>7</sub>H<sub>8</sub>O<sub>2</sub>)  
415 and lower (relative) EF for aromatics for the peat samples (PM, PF) is consistent with the low temperature pyrolysis and  
high expected lignin content for these fuels (Stockwell et al., 2015; Dyakonov et al., 2008). Additional discrepancies between  
aircraft-derived wildfire EF vs. laboratory EF (this study and others) may also be attributed to differences associated with aged  
vs. fresh emissions (Permar et al., 2021).

To further explore VOC emission variability between fuel types, principal component analysis (PCA) was performed using  
420 the mean VOC EF data for the all fuel types as inputs, with methods and results described and presented in SI Section S7 (Fig.  
S6). The PCA results further confirm that although MCE plays a dominant role, additional factors (e.g., fuel moisture content)  
are required to explain VOC emissions variability. The PCA results also emphasize the unique emission behavior of both the  
dry and wet peat fuels (PM, PF).

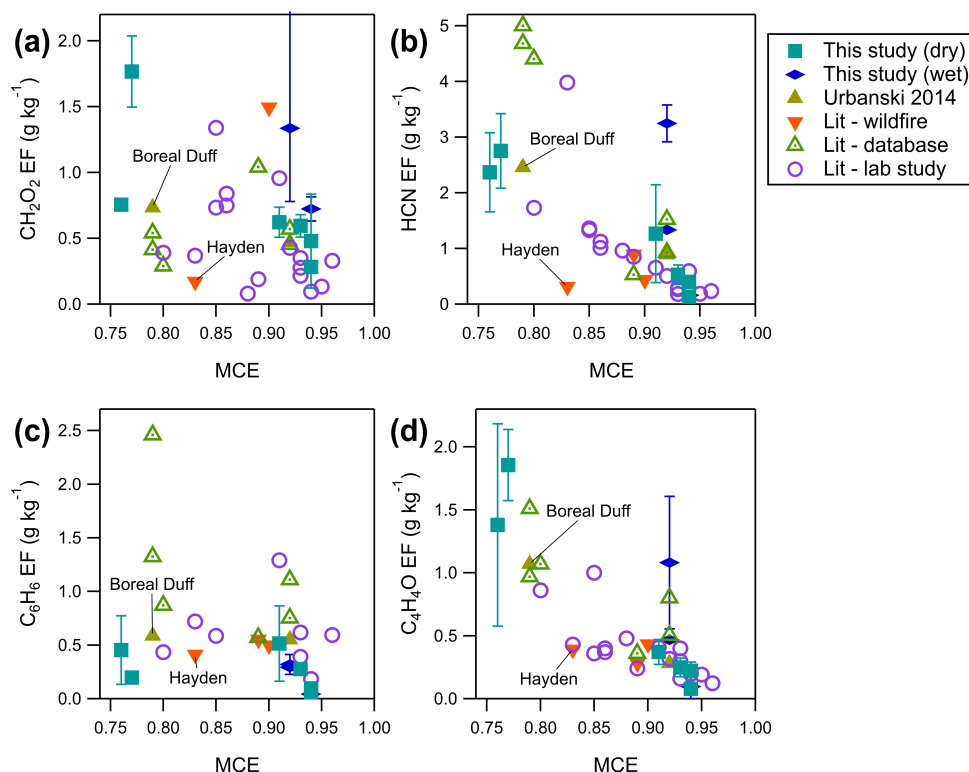


**Figure 5.** Mean overall EF for a) CH<sub>2</sub>O<sub>2</sub> (formic acid), b) HCN (hydrogen cyanide), c) C<sub>6</sub>H<sub>6</sub> (benzene), and d) C<sub>4</sub>H<sub>4</sub>O (furan) as a function of mean fire-integrated MCE for low moisture content fuels (PM, PF, SM, PN, GR, MU; teal squares) and wet fuels (PM, PF, MU; blue diamonds). Error bars represent the standard deviation of the mean. Also shown are EFs from wildfire studies (orange triangles) (Hayden et al., 2022; Simpson et al., 2011; Permar et al., 2021), laboratory studies (purple circles), (Koss et al., 2018; Yokelson et al., 2013; Stockwell et al., 2015; Bertschi et al., 2003; Selimovic et al., 2018) and EF databases/compilations (open green triangles) (Akagi et al., 2011; Andreae, 2019; Binte Shahid et al., 2024), including Urbanski (2014) “Boreal Forest Duff” and “Wildfire Boreal Forest” (solid green triangles) where available. See SI Section S5 for more information on the literature studies.

### 3.5 Nitrogen-containing species

425 Biomass burning is an important source of Nr to the atmosphere. Although total Nr was not measured during this study, analysis of the available nitrogen-containing inorganic and organic gas-phase species reveals important differences amongst the fuels. Fig. 6a shows the  $\sum$ Nr EF in units of g N kg<sup>-1</sup> from nitrogen-containing inorganic (NO, NO<sub>2</sub>, HONO, NH<sub>3</sub>) and organic (HCN, HNCO, C<sub>2</sub>H<sub>3</sub>N - acetonitrile, C<sub>6</sub>H<sub>5</sub>NO<sub>3</sub> - nitrophenol, and OTHER, which includes C<sub>3</sub>H<sub>3</sub>NO<sub>2</sub> - cyanoacetic acid, C<sub>2</sub>H<sub>3</sub>NO - glycolic acid nitrile/methyl isocyanate, C<sub>2</sub>H<sub>5</sub>NO<sub>3</sub>- nitroethanol, and C<sub>7</sub>H<sub>5</sub>N - benzonitrile) species as a function of biomass type. Fig. 6b shows the percentage contribution of the measured species to the  $\sum$ Nr EF. The fuel nitrogen (N) content (Table 1) ranged from 0.27 % (MU) to 1.2 % (GR) and is considerably more variable than fuel carbon content. The measured  $\sum$ Nr EFs spanned from 0.71 g N kg<sup>-1</sup> for MU (dry) to 5.18 g N kg<sup>-1</sup> for PM (dry). These values indicate that, at most, ~ 51 % of the fuel N is accounted for in PM (dry) (1.02 % fuel N), whereas as little as ~ 17 % was accounted for in GR (dry),



assuming the same N % in the consumed fuel. These ranges are consistent with other studies (Watson et al., 2019). From a  
435 total N perspective, approximately half of fuel N is typically emitted as N<sub>2</sub> (Burling et al., 2010; Roberts et al., 2020; Lindaas  
et al., 2021b; Goode et al., 1999; Kuhlbusch et al., 1991), and the low closure of the N budget from the high MCE fuels is  
consistent with significant denitrification to N<sub>2</sub> (and N<sub>2</sub>O) during high-temperature combustion. The low  $\sum$ Nr EF for MU is  
consistent with the low fuel N content (0.27 %) and low fuel nitrogen to carbon ratio (N/C) of 0.01, while the moderate  $\sum$ Nr  
EF for GR is likely due to its higher N content (1.21 %) and high fuel N/C ratio (0.03), as other studies have found that fuels  
440 with higher N content typically have higher  $\sum$ Nr emissions (Turetsky et al., 2011; Lindaas et al., 2021b) with a higher fraction  
of N-containing VOC (Coggon et al., 2016). However, SI Fig. S8 (a) and (b) show that fuel N content on its own cannot fully  
explain individual Nr EF and  $\sum$ Nr EF.

Similar to the carbon budget analysis, the N budget lacks contributions from unreactive nitrogen (N<sub>2</sub>, N<sub>2</sub>O) as well as  
some unmeasured Nr species (HNO<sub>3</sub> and other NO<sub>y</sub>, other N-containing organics such as amines, amides, nitro-compounds,  
445 nitriles, and N-heterocyclic compounds), particle-bound N, and N in remaining ash, and full closure is not expected (Roberts  
et al., 2020; Hayden et al., 2022; Lindaas et al., 2021b; Goode et al., 1999). However, laboratory studies (Burling et al., 2010;  
Roberts et al., 2020), and aircraft wildfire studies (Hayden et al., 2022; Lindaas et al., 2021b) consistently find that NO, NO<sub>2</sub>,  
HONO, HNCO, HCN, C<sub>2</sub>H<sub>3</sub>N, and NH<sub>3</sub>, all of which were measured in this study, are the major contributors to Nr, with a  
minor contribution from other N-containing VOC (< 5-10 %) and little to no measurable HNO<sub>3</sub>. In the FIREX-2016 laboratory  
450 campaign (Roberts et al., 2020), unexplained Nr amounted to ~ 15 % and was attributed to low-volatility and/or particle-bound  
nitrogen, similar to Hayden et al. (2022), who found that particle-bound nitrogen (NH<sub>4</sub><sup>+</sup>, NO<sub>3</sub><sup>-</sup>) contributed ~ 23 % to the  
total measured Nr from a boreal wildfire. Measurements of fine particle ammonium and nitrate by a Soot Particle Aerosol Mass  
Spectrometer will be addressed in a subsequent BBCan paper.

Fig. 6 shows that peat-associated fuels PF (dry) and PM (dry) exhibit elevated emissions and relative contributions from  
455 reduced N species (HCN, NH<sub>3</sub>, C<sub>2</sub>H<sub>3</sub>N), which are primarily formed from fuel pyrolysis, and low emissions and relative  
contributions from oxidized N species (HONO, NO<sub>2</sub>, NO), which are formed in the flame through rapid oxidation of small N-  
containing compounds, while the opposite is true for the flaming-dominated fuels (GR and MU). Hanashiro Moraes et al. (2026)  
also confirm that NO<sub>x</sub> and NH<sub>3</sub> emissions are more closely related to flaming CO<sub>2</sub> and smoldering CO, respectively, while  
Fig. 1 shows that HCN emissions are associated with both flaming and smoldering CO. The distribution of Nr species across  
460 fuels and combustion behavior is roughly consistent with the positive matrix factorization analysis performed by Roberts et al.  
(2020) on Nr emissions from coniferous fuels (FIREX-2016) that found three factors: a combustion (flaming) factor dominated  
by NO, NO<sub>2</sub>, and HONO; a high-temperature pyrolysis factor dominated by HCN, HNCO, and nitriles; and a low-temperature  
pyrolysis factor dominated by NH<sub>3</sub>, amines, amides, and heterocyclics, similar to the two-factor solution of Sekimoto et al.  
(2018). High NH<sub>3</sub> and HCN EFs and low NO<sub>x</sub> EFs, which are observed for PM and PF (Fig. 6a), are particularly characteristic  
465 of peat fuels that do not sustain flaming combustion and burn at lower temperatures (Watson et al., 2019; Yokelson et al., 1997;  
Goode et al., 2000) and the pyrolysis of nitrogen heterocycles, which are typically enriched in organic soils compared to  
woody and leafy fuels, is associated with high HCN emissions (Sekimoto et al., 2018). They are also consistent with top-down



estimates demonstrating unexpectedly high  $\text{NH}_3$  emissions from boreal forest fires (Chen et al., 2025). We note that the PM sample representing peat impacted by human activity had higher  $\sum \text{Nr}$  and  $\text{NH}_3$  EFs compared to the natural sample (PF).

470 While the EF for reduced N species follows an inverse relationship with MCE (Fig. 6c), similar to other VOC, as observed here (Fig. 5 and S5) and elsewhere (Lindaas et al., 2021b), the EF for oxidized N species generally increases with increasing MCE (Fig. 6b). The higher MCE value likely reflects higher combustion temperatures, which promote more efficient oxidation and hence greater emissions of NO,  $\text{NO}_2$ , and HONO (Lindaas et al., 2021a). Again, MU, with its low N fuel content, exhibits distinct behavior, with low EF for these oxidized species compared to other fuels with similar MCE. A relatively weak corre-

475 lation for the oxidized nitrogen species has been observed by others and is likely due, in part, to variable fuel N, and indeed the correlation for HONO and NO is found to improve slightly when scaling the EF by fuel N or by  $\sum \text{Nr}$  (see SI. Figs. S8c-e) (Burling et al., 2010). Moreover, flame chemistry involving reactions of HNCO, HCN,  $\text{NH}_3$ , HONO, and  $\text{NO}_x$  is highly complex, and emissions of these species may be due to multiple, temperature-dependent pathways, resulting in non-linear variation in EF with MCE (Burling et al., 2010; Roberts et al., 2020; Goode et al., 2000). Constraining emissions of oxidized nitrogen

480 species is important given that  $\text{NO}_x$  strongly influences photochemical processing in wildfire plumes, which is often expected to operate under  $\text{NO}_x$ -limited conditions (Jaffe and Wigder, 2012; Lin et al., 2024; Voulgarakis and Field, 2015). HONO, a key photolytic precursor of hydroxyl radicals that initiate atmospheric oxidation, significantly influences the chemical evolution of smoke as it disperses (Stutz et al., 2010; Kleffmann, 2007).

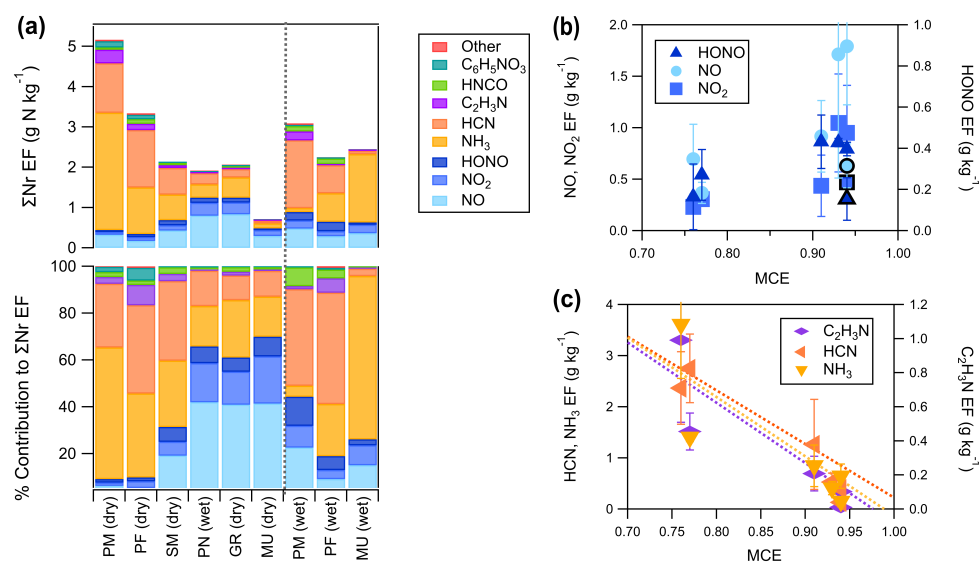


**Figure 6.** (a) EF of Nr species ( $\text{g N kg}^{-1}$ ) on the top panel and their % contribution to  $\sum \text{Nr}$  on the bottom panel; (b) NO,  $\text{NO}_2$ , and HONO EFs ( $\text{g kg}^{-1}$ ); and (c) HCN,  $\text{NH}_3$ , and  $\text{C}_2\text{H}_3\text{N}$  EFs ( $\text{g kg}^{-1}$ ) as a function of fire-integrated MCE for the low-moisture content fuels [MU (dry), GR (dry), SM (dry), PN (wet), PF (dry), PM (dry)]. MU (dry) EFs are outlined in black in Fig. 6b. Error bars represent the standard deviation of the mean. The dashed lines in Fig. 6(c) are linear fits to the data.



The impact of fuel moisture content on the Nr emission profile is also evident in Fig. 6a when comparing dry PF, PM, and  
485 MU fuels with their undried counterparts. The HONO/NO<sub>x</sub> ratio is observed to increase for the wet peat fuels, possibly due  
to the flame chemistry involving NO<sub>2</sub> hydrolysis to form HONO (Roberts et al., 2020). Consistent with this, HONO EFs are  
highest for PF (wet), reaching 0.78 g kg<sup>-1</sup> followed by PM (wet) at 0.70 ± 0.10 g kg<sup>-1</sup>. In addition, the wet peat fuels, which  
burned a small fraction of fuel mainly by flaming combustion in this study, exhibit higher relative contributions of HCN and  
HNCO, which are characteristic of high-temperature pyrolysis (Roberts et al., 2020). The wet peat fuels have higher HCN/NH<sub>3</sub>  
490 than their dry counterparts, which is contrary to the finding of Yokelson et al. (1997) that drier organic soils/peats exhibit higher  
HCN/NH<sub>3</sub> ratios, although a large variation in HCN/NH<sub>3</sub> was observed across fuels in that study. The difference in behavior is  
likely related to the fact that the wet peat fuels did not sustain smoldering combustion. MU (wet), which has a relatively similar  
VOC profile compared to MU (dry), has a much higher NH<sub>3</sub> EF compared to its dry counterpart, further indicating that even  
small differences in fuel moisture-content can impact Nr emissions.

495 With respect to prior studies, HNCO and C<sub>2</sub>H<sub>3</sub>N EFs largely fall within reported ranges (Fig. 2) with EFs consistent with  
the literature EF vs. MCE relationships (Figs. S5b and f). HCN is consistently elevated in peat relative to non-peat fuels but  
still remains within the typical literature range. The HCN EF for the dry peat fuels, PM (2.4 ± 0.7 g kg<sup>-1</sup>) and PF (2.8 ±  
0.8 g kg<sup>-1</sup>), are in good agreement with one another, the Urbanski (2014) “Boreal Forest Duff” HCN EF (2.5 ± 0.8 g kg<sup>-1</sup>)  
(Fig. 6b) and a recent laboratory study of peat from an Alaskan black spruce forest (2.3 ± 0.3 g kg<sup>-1</sup>), but intermediate to the  
500 reported range of HCN EF for other peat fuels (~ 0.7 - 6 g kg<sup>-1</sup>) (Watson et al., 2019). The low HCN EF for MU (0.13 ± 0.09  
g kg<sup>-1</sup>) is consistent with the low HCN EF for Alaskan black spruce canopy (0.24 ± 0.07 g kg<sup>-1</sup>)<sup>67</sup> and Albertan Jack pine  
and black spruce needles and woody debris (0.097 ± 0.067 g kg<sup>-1</sup>) (Urbanski et al., 2022). HCN and C<sub>2</sub>H<sub>3</sub>N are also often  
used as biomass burning markers/tracers (Goode et al., 1999).

Interestingly, for the dry peat fuels, we observed relatively high but variable EF (ranging from below the detection limit to  
505 a maximum of 1.57 g kg<sup>-1</sup> and 1.94 g kg<sup>-1</sup> for individual burns of PM and PF, respectively) for C<sub>6</sub>H<sub>5</sub>NO<sub>3</sub> measured from  
the I-CIMS that we assign as nitrophenol. These EFs are significantly higher than the nitrophenol EFs from the other low  
moisture-content fuels, ranging from 0.003 g kg<sup>-1</sup> for SM up to 0.065 g kg<sup>-1</sup> for PN (see Table 1), which are more consistent  
with other studies (Wang et al., 2017). In addition to being toxic, nitrophenols can contribute to brown carbon (Mohr et al.,  
2013) and thus influence the radiative budget.

510 This study demonstrates that ∑Nr emissions from Canadian boreal surface and ground fuels, as well as the Nr speciation  
profile, particularly with respect to the relative contributions from oxidized and reduced species, are influenced by combustion  
conditions (i.e., MCE and/or pyrolysis temperature), total fuel N content, and moisture.

### 3.6 Implications and summary

#### 3.6.1 Implications for wildfire emissions in CFFEPS

515 Due to its relevance to Canadian boreal wildfires, the process of estimating emissions using CFFEPS is briefly described here.  
CFFEPS is the wildfire emissions model in ECCC’s operational air quality forecast system (Boutzis et al., 09 Dec 2025). Fire



emissions are calculated as the product of tabulated EFs ( $\text{g kg}^{-1}$ ), the estimated fire burn area ( $\text{m}^{-2}$ ) and the TFC ( $\text{kg}$  of dry biomass  $\text{m}^{-1}$ ). Fuel consumption in CFFEPS is estimated based on the Canadian Forest FBP system (Natural Resources Canada, 2025b) driven by fire weather conditions for 14 pre-defined FBP fuel types. Combustion is divided into three stages: flaming, smoldering, and residual combustion (details on allocation factors in SI Section S9). Although CFFEPS allows fuel-specific EFs, the current application uses a single set of EFs for all fuels for a given combustion stage.

At present, CFFEPS includes tabulated EFs for  $\text{PM}_{10}$ ,  $\text{PM}_{2.5}$ , CO,  $\text{CH}_4$ ,  $\text{NMOC}_G$ ,  $\text{NO}_X$ ,  $\text{NH}_3$ , and  $\text{SO}_2$  other model-required species. Emissions of  $\text{NMOC}_G$  are further speciated to individual VOC using emission speciation profiles for flaming and smoldering/residual combustion, assuming constant MCE values of 0.92 and 0.79, respectively, following Urbanski (2014) and EPA SPECIATEv4.5; henceforward the ‘CFFEPS profiles’. This is a single set of EF profiles for all fuel types, and as described in the Introduction, the profiles are, for the most part, not based on studies of Canadian boreal wildfires or fuels. Yet, our study adds to the body of literature that demonstrates that  $\text{NMOC}_G$  emission magnitude and speciation profile (i.e., VOC EFs) are impacted by fuel type, combustion behavior, and fuel moisture.

The flaming, smoldering, and residual  $\text{NMOC}_G$  EF used in CFFEPS are  $19.85 \text{ g kg}^{-1}$ ,  $33.87 \text{ g kg}^{-1}$ , and  $56.08 \text{ g kg}^{-1}$ , respectively (Chen et al., 2019). Revising our NMOC EF in  $\text{g C kg}^{-1}$  to  $\text{NMOC}_G$  EF in  $\text{g kg}^{-1}$  for comparison requires knowledge of the NMOC composition and/or mean MW. For a rough comparison, we use the conversion from Hayden et al. (2022) (mean MW of  $100 \text{ g mol}^{-1}$  and mean carbon number of 6) to obtain  $\text{NMOC}_G$  EF listed in Table 1. The  $\text{NMOC}_G$  EF for our study, along with the Hayden et al. (2022) ( $\text{MCE} = 0.82$ ,  $\text{NMOC}_G = 39.9 \pm 5.8 \text{ g kg}^{-1}$ ) and Urbanski (2014)  $\text{NMOC}_G$  EF for “Wildfire Boreal Forest” ( $\text{MCE} = 0.92$ ,  $\text{NMOC}_G = 23.15 \pm 13.13 \text{ g kg}^{-1}$ ) and “Boreal Forest Duff” ( $\text{MCE} = 0.79$ ,  $\text{NMOC}_G = 54.33 \pm 42.84 \text{ g kg}^{-1}$ ), are plotted as a function of MCE in Fig. S9. The high total  $\text{NMOC}_G$  EFs for the dry peat fuels [PM ( $45.2 \pm 3.4 \text{ g kg}^{-1}$ ), PF ( $56.9 \pm 5.4 \text{ g kg}^{-1}$ )] lie between the CFFEPS  $\text{NMOC}_G$  EFs for smoldering and residual combustion, near the Urbanski (2014) NMOG EF, and above the Hayden et al. (2022) NMOG EF, but are consistent with the observed inverse linear relationship between  $\text{NMOC}_G$  and MCE ( $R^2 = 0.82$ ) (Fig. S9). Therefore, while our results suggest that total  $\text{NMOC}_G$  emissions may be underestimated by CFFEPS for smoldering peat fires, the strong  $\text{NMOC}_G$ -MCE relationship ( $R^2 = 0.82$ ) we observe may be a useful predictor for total  $\text{NMOC}_G$  emissions. On the other hand, we found that the overall relationship between NMOC (or  $\text{NMOC}_G$ ) EF and MCE for MU (dry) deviated from that of the other fuels (Fig. 3 and Fig. S9), and the total  $\text{NMOC}_G$  EF for MU (dry) ( $5.5 \pm 3.0 \text{ g kg}^{-1}$ ) obtained in this study is significantly lower than the CFFEPS  $\text{NMOC}_G$  for flaming combustion.

Trace gas EFs for PM (dry) and PF (dry) are plotted vs. the CFFEPS smoldering/residual profile EFs in Fig. 7a. The figure includes EF for speciated VOC from this work (solid symbols) as well as other trace gas species (open symbols) reported in the overview paper (Moraes et al., 7 May 2026). The speciated VOC EF for the peat fuels are similar to or slightly lower than the corresponding CFFEPS profile EFs, despite the low MCE, with the exception of some CH compounds (e.g., styrene, isoprene). The deviation from linearity indicates differences in interspecies ERs compared to the literature profiles. We also note that differences between our study EFs and the literature EFs could be due to limitations in compound assignment as discussed above (Section 2.2). These differences suggest that the current VOC speciation profile used in CFFEPS, and subsequent assignment



of individual VOC to lumped species in simplified atmospheric chemical mechanisms may not adequately capture emissions from peat fuels that dominate the boreal forests fuel types in Canada.

Incorporating Canadian-specific EF from this study, as well as recent studies such as Hayden et al. (2022), into emission inventories/databases will improve atmospheric model performance for boreal wildfire and prescribed burning scenarios and provide a more robust basis for air quality and climate assessments. A similar comparison as in Fig. 7a is made between this study and Hayden et al. (2022), aircraft study in Fig. 7b. Overall, the VOCs EF (solid symbols) in this study for peat fuels are consistently similar to or higher than those reported in Hayden et al. (2022), with the exception of only a few compounds (e.g.,  $C_3H_4O_3$  - pyruvic acid), consistent with the higher degree of smoldering combustion for the peat fuels (i.e., low MCE compared to the wildfire). EFs for inorganic nitrogen species (NO, HONO,  $NH_3$ ) from the peat-associated fuels are found to be significantly higher, likely related to the measurement of fresh emissions (our study) vs. aged emissions (Hayden et al., 2022). Future work to improve emissions in CFFEPS and other wildfire emissions models should focus on deriving EF from boreal biomass types for a greater number of VOC species, particularly low-molecular weight compounds (e.g., C1-C2 VOC) and I/SVOC, compound classes that are both expected to contribute significantly to the total NMOC (Hayden et al., 2022).

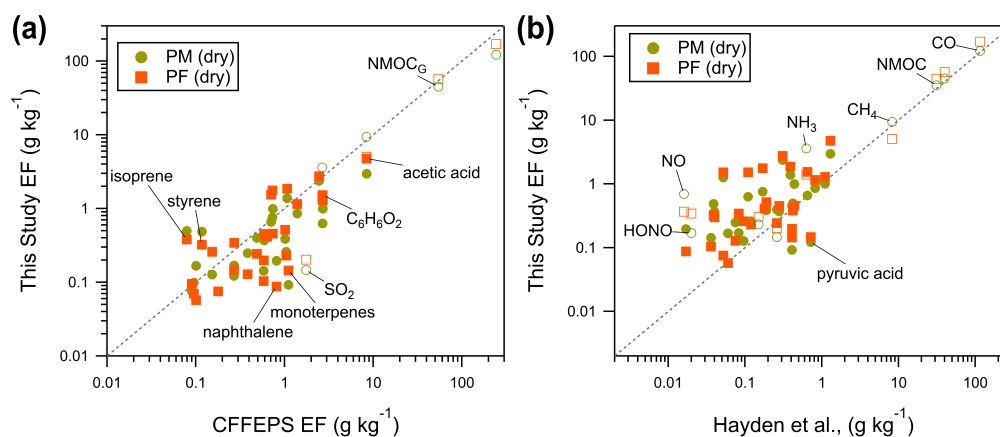


**Figure 7.** EF ( $g\ kg^{-1}$ ) for 32 VOC (solid symbols) and other trace gas species (open symbols) (Moraes et al., 7 May 2026) for dry peat fuels [PM (dry) - green circle, PF (dry) - orange squares] compared to (a) CFFEPS EFs for residual/smoldering combustion of boreal forest duff/organic soil from Urbanski (2014) and (b) EFs measured by aircraft for a boreal wildfire from Hayden et al. (2022). The dotted line is the 1:1 line. Error bars are omitted for clarity. The identities of select species are shown to highlight key differences/similarities.

### 3.7 Summary

Controlled laboratory burns of six Canadian surface and ground fuels were conducted to derive EFs and to systematically assess how variations in fuel characteristics and combustion behavior shape trace gas emissions. Coupling measurements of speciated VOCs with concurrent observations of major carbon species ( $CO_2$ , CO,  $CH_4$ ), total NMOC, and Nr species (HONO,  $NH_3$ ,  $NO_x$ ) enabled improved understanding of gas-phase carbon and nitrogen emissions associated with boreal wildfires. Canadian boreal peat fuels (i.e., peat with surface mulch, peat with moss) burn with very low MCE and are prone to residual smoldering combustion, resulting in very high NMOC and CO emissions compared to other fuel types. We found



that total NMOC emissions were well-described by MCE and with a NMOC-VOC relationship independent of fuel type, with the exception of MU, which has very low NMOC emissions. While the relationship between individual VOC EF and MCE was found to be well-described and relatively independent of fuel identity for several VOC species, this was not universally observed, indicating that predicting EF based on MCE may not be appropriate in all cases (Yokelson et al., 2013; Andreae, 575 2019; Sekimoto et al., 2018). Differences in emissions behaviour between the peat fuels suggest that human disturbance may affect wildfire emissions from peatlands.

Wildfires consume a diverse combination of surface and crown fuels, with combustion conditions and moisture content in wildland vegetation fluctuating with climate, meteorological conditions, and fuel structure and arrangement. While controlled burn studies such as this one provide key insights, further aircraft studies targeting Canadian boreal wildfires are also needed 580 to capture real-world emissions. Ultimately, integrating high-resolution laboratory data with field measurements will enable more robust simulations of biomass burning emissions and improve predictions of air quality and climate impacts under diverse combustion scenarios.

Table 1: Fuel properties and emission factors.

Parameters	PN (wet)		MU (dry)		MU (wet)		GR (dry)		PF (dry)		PF (wet)		PM (dry)		PM (wet)		SM (dry)		
<sup>a</sup> FBP fuel type	C-7 Litter		C-2 (Boreal Spruce) upper duff				O-1 Grass		<sup>b</sup> C-2 (Boreal spruce) upper duff								M-2 (Boreal mixedwood) litter		
<sup>c</sup> Number of replicates	2		4		2		4		3		1		4		3		5		
Elemental composition (%)	C(49.27) N(0.55)		C(47.28) N(0.27)				C(43.37) N(1.21)		C(48.27) N(1.07)		C(47.39) N(1.02)		C(44.39) N(1.07)						
	Mean	SD	Mean	SD	Mean	SD	Mean	SD	Mean	SD	Mean	SD	Mean	SD	Mean	SD	Mean	SD	
Moisture (%)	12.98	0.14	4.15	–	7.45	–	19.81	0.80	7.56	0.19	51.43	–	15.16	1.96	100.36	0.11	13.71	0.89	
Fuel mass (kg)	0.050	0.013	0.197	0.021	0.204	0.026	0.095	0.046	0.089	0.019	0.011	–	0.181	0.061	0.018	0.005	0.065	0.027	
MCE	0.93	0.01	0.94	0.02	0.94	0.02	0.94	0.004	0.77	0.02	0.92	–	0.76	0.07	0.92	0.01	0.91	0.01	
Duration (min)	19.00	7.55	47.50	15.59	41.00	11.31	18.50	12.08	86.46	17.04	28.00	–	126.88	8.98	42.00	6.93	31.70	6.08	
NMOC (g C kg <sup>-1</sup> )	17.18	1.72	4.28	2.32	8.13	3.58	14.11	2.87	44.44	4.25	17.53	–	35.09	2.67	27.47	11.31	24.17	5.46	
<sup>d</sup> ∑NMOC <sub>G</sub> (g kg <sup>-1</sup> )	21.99	2.20	5.48	2.97	10.55	4.37	18.10	3.73	56.88	5.44	22.44	–	45.22	3.44	35.16	14.48	30.93	6.98	
∑VOCs (g kg <sup>-1</sup> )	5.64	0.56	1.95	0.43	2.31	0.38	3.75	0.21	24.75	2.01	8.90	–	20.57	2.43	18.30	2.58	9.92	1.23	
<b>Emission factors (g kg<sup>-1</sup>)</b>																			
Mass	Formula	Mean	SD	Mean	SD	Mean	SD	Mean	SD	Mean	SD	Mean	SD	Mean	SD	Mean	SD	Mean	SD
27.01	HCN	0.53	0.17	0.13	0.09	0.16	0.02	0.40	0.05	2.75	0.67	1.34	–	2.37	0.71	3.24	0.33	1.27	0.88
41.03	C <sub>2</sub> H <sub>3</sub> N	–	–	0.01	0.004	0.005	0.01	0.10	0.01	0.46	0.11	0.09	–	0.99	0.48	0.65	0.62	0.21	0.10
43.01	HNCO	0.08	0.02	0.02	0.01	0.02	0.004	0.12	0.02	0.34	0.10	0.41	–	0.17	0.03	0.40	0.15	0.17	0.08
44.03	C <sub>2</sub> H <sub>4</sub> O	–	–	0.06	0.05	0.01	0.004	0.24	0.05	1.29	0.16	–	–	1.00	–	0.39	0.27	0.58	0.07
46.01	CH <sub>2</sub> O <sub>2</sub>	0.59	0.09	0.48	0.36	0.72	0.09	0.28	0.01	1.77	0.27	1.34	–	0.76	0.03	2.56	1.78	0.62	0.11
47.00	HONO	0.43	0.02	0.15	0.10	0.20	0.07	0.40	0.03	0.27	0.12	0.78	–	0.16	0.16	0.70	0.10	0.43	0.13
56.03	C <sub>3</sub> H <sub>4</sub> O	0.29	–	0.04	0.02	0.05	0.06	0.25	0.06	0.45	0.06	0.21	–	0.37	0.23	0.38	0.12	0.27	0.02
57.02	C <sub>2</sub> H <sub>3</sub> NO	0.001	–	0.0004	–	–	–	0.001	0.06	0.003	0.002	0.002	–	0.003	–	0.01	0.0002	0.004	–
58.04	C <sub>3</sub> H <sub>6</sub> O	0.12	–	0.03	0.001	–	–	0.21	0.02	1.15	0.21	–	–	0.86	0.33	0.37	0.07	0.34	0.04
60.02	C <sub>2</sub> H <sub>4</sub> O <sub>2</sub>	0.28	0.10	0.16	0.04	0.20	0.20	0.39	0.14	4.75	0.45	1.41	–	2.95	1.75	1.91	1.37	1.67	0.51
68.03	C <sub>4</sub> H <sub>4</sub> O	0.25	0.07	0.08	0.03	0.10	0.10	0.22	0.07	1.86	0.28	0.47	–	1.38	0.80	1.08	0.53	0.37	0.10
68.06	C <sub>5</sub> H <sub>8</sub>	0.10	–	–	–	–	–	0.09	0.01	0.38	0.06	–	–	0.50	0.28	0.31	0.26	0.22	0.02
70.04	C <sub>4</sub> H <sub>6</sub> O	0.02	–	0.04	0.01	0.03	0.03	0.21	0.04	0.52	0.07	0.17	–	0.39	0.23	0.34	0.16	0.24	0.01
72.02	C <sub>3</sub> H <sub>4</sub> O <sub>2</sub>	0.14	0.05	0.06	0.04	0.11	–	0.05	0.02	0.26	0.20	0.21	–	0.13	0.03	0.45	0.26	0.19	0.07
72.06	C <sub>4</sub> H <sub>8</sub> O	–	–	0.01	0.004	0.01	–	0.07	0.01	0.41	0.06	–	–	0.43	0.20	0.18	0.10	0.11	0.01
74.00	C <sub>2</sub> H <sub>2</sub> O <sub>3</sub>	–	–	0.0001	–	–	–	–	–	0.02	–	–	–	0.001	–	–	–	0.001	0.001
76.02	C <sub>2</sub> H <sub>4</sub> O <sub>3</sub>	0.01	0.01	0.02	0.02	0.03	0.01	0.001	0.001	0.10	0.14	0.03	–	0.08	0.01	0.07	0.08	0.01	0.02
78.05	C <sub>6</sub> H <sub>6</sub>	0.28	–	0.06	0.03	0.04	0.03	0.10	0.02	0.20	0.05	0.29	–	0.45	0.32	0.32	0.09	0.51	0.35

Continued on next page



Table 1 (continued)

Parameters		PN (wet)		MU (dry)		MU (wet)		GR (dry)		PF (dry)		PF (wet)		PM (dry)		PM (wet)		SM (dry)	
Mass	Formula	Mean	SD	Mean	SD	Mean	SD	Mean	SD	Mean	SD	Mean	SD	Mean	SD	Mean	SD	Mean	SD
85.02	C <sub>3</sub> H <sub>3</sub> NO <sub>2</sub>	0.003	0.002	0.0003	0.0002	0.002	–	0.0001	–	–	–	0.001	–	–	–	0.004	–	0.0003	0.0004
88.02	C <sub>3</sub> H <sub>4</sub> O <sub>3</sub>	0.20	0.14	0.23	0.15	0.19	0.10	0.04	–	0.15	0.11	0.58	–	0.12	0.13	1.39	0.19	0.12	0.06
88.05	C <sub>4</sub> H <sub>8</sub> O <sub>2</sub>	–	–	–	–	–	–	0.07	–	–	–	–	–	0.40	0.10	–	–	0.12	0.08
90.03	C <sub>3</sub> H <sub>6</sub> O <sub>3</sub>	0.07	0.01	0.01	0.003	0.06	0.06	0.02	0.01	0.11	0.10	0.36	–	0.11	0.00	0.38	0.25	0.06	0.04
91.03	C <sub>3</sub> H <sub>5</sub> NO <sub>2</sub>	0.003	–	0.001	–	0.01	–	0.0004	–	0.01	0.01	0.01	–	–	–	0.04	–	0.003	–
92.06	C <sub>7</sub> H <sub>8</sub>	0.18	0.08	0.02	0.01	0.01	0.01	0.06	0.01	0.24	0.04	0.13	–	0.40	0.17	0.19	0.14	0.23	0.12
94.04	C <sub>6</sub> H <sub>6</sub> O	0.11	0.02	0.02	0.01	0.01	0.01	0.05	0.01	0.23	0.04	0.11	–	0.26	0.12	0.14	0.07	0.10	0.04
96.02	C <sub>5</sub> H <sub>4</sub> O <sub>2</sub>	0.16	0.18	0.06	0.02	0.09	0.09	0.20	0.07	1.54	0.16	0.38	–	0.66	0.37	0.73	0.30	0.29	0.09
100.09	C <sub>6</sub> H <sub>12</sub> O	–	–	0.001	0.0001	0.001	–	0.003	0.0002	0.04	0.00	–	–	0.05	0.03	0.03	0.03	0.02	0.002
102.10	C <sub>5</sub> H <sub>10</sub> O <sub>2</sub>	–	–	–	–	–	–	–	–	–	–	–	–	–	–	–	–	0.02	0.02
103.04	C <sub>7</sub> H <sub>5</sub> N	0.02	0.01	0.005	0.003	0.002	0.002	0.01	0.001	0.06	0.01	0.04	–	0.17	0.06	0.10	0.07	0.06	0.03
104.05	C <sub>4</sub> H <sub>8</sub> O <sub>3</sub>	0.01	0.001	0.003	0.003	0.004	0.004	0.001	0.001	0.03	0.02	0.02	–	0.04	0.01	0.05	0.03	0.01	0.01
104.06	C <sub>8</sub> H <sub>8</sub>	0.28	0.38	0.04	0.02	0.03	0.03	0.10	0.004	0.32	0.07	0.30	–	0.49	0.31	0.36	0.17	0.53	0.34
106.04	C <sub>7</sub> H <sub>6</sub> O	0.06	0.05	0.01	0.005	0.01	0.005	0.04	0.01	0.10	0.02	0.03	–	0.14	0.08	0.11	0.09	0.08	0.03
106.08	C <sub>8</sub> H <sub>10</sub>	0.09	0.002	0.01	0.003	0.004	0.005	0.03	0.002	0.13	0.02	0.08	–	0.25	0.08	0.07	0.06	0.10	0.03
108.06	C <sub>7</sub> H <sub>8</sub> O	0.08	0.06	0.03	0.01	0.02	0.02	0.07	0.01	0.30	0.08	0.08	–	0.37	0.16	0.15	0.07	0.11	0.02
110.04	C <sub>6</sub> H <sub>6</sub> O <sub>2</sub>	0.13	–	0.03	0.01	0.03	0.03	0.13	0.03	1.52	0.13	0.31	–	0.63	0.33	0.41	0.19	0.19	0.06
116.05	C <sub>5</sub> H <sub>8</sub> O <sub>3</sub>	0.06	0.03	0.03	0.03	0.05	0.05	0.03	0.01	0.22	0.16	0.16	–	0.21	0.07	0.28	0.19	0.09	0.07
116.08	C <sub>6</sub> H <sub>12</sub> O <sub>2</sub>	–	–	–	–	–	–	–	–	–	–	–	–	0.09	0.001	–	–	0.01	0.01
118.06	C <sub>5</sub> H <sub>10</sub> O <sub>3</sub>	0.003	0.0003	0.0004	0.0001	0.001	–	0.001	0.001	0.003	0.003	0.001	–	0.004	0.003	0.0004	–	0.003	0.002
120.09	C <sub>6</sub> H <sub>12</sub>	0.06	0.06	0.003	0.001	0.002	–	0.01	0.002	0.08	0.01	0.02	–	–	–	–	–	0.04	0.004
124.05	C <sub>7</sub> H <sub>8</sub> O <sub>2</sub>	0.22	0.19	0.17	0.12	0.23	0.23	0.03	0.004	1.52	1.27	0.06	–	1.26	0.72	0.46	0.40	0.25	0.24
128.06	C <sub>10</sub> H <sub>8</sub>	0.60	–	0.04	0.02	0.03	0.02	0.03	0.01	0.09	0.03	0.18	–	0.20	0.18	0.30	0.12	0.36	0.28
130.06	C <sub>6</sub> H <sub>10</sub> O <sub>3</sub>	0.01	0.01	0.004	0.004	0.01	0.01	0.003	–	0.04	0.03	0.02	–	0.04	0.02	0.05	0.02	0.01	0.01
130.10	C <sub>7</sub> H <sub>14</sub> O <sub>2</sub>	–	–	–	–	–	–	0.000	–	–	–	–	–	0.10	–	–	–	0.02	0.02
136.13	C <sub>10</sub> H <sub>16</sub>	0.38	0.09	0.01	0.002	–	–	0.01	0.01	0.14	0.05	–	–	0.09	0.08	0.08	0.06	0.27	0.02
139.06	C <sub>6</sub> H <sub>5</sub> NO <sub>3</sub>	0.09	0.06	0.02	–	0.04	0.03	0.07	0.05	1.12	1.16	–	–	1.57	–	0.25	0.08	–	–
184.11	C <sub>10</sub> H <sub>16</sub> O <sub>3</sub>	0.003	0.002	0.001	0.001	0.0002	–	0.0001	–	0.005	0.004	0.001	–	0.004	0.003	0.003	–	0.002	0.002
204.19	C <sub>15</sub> H <sub>24</sub>	0.14	–	0.0004	0.0002	0.002	–	0.003	0.001	0.07	0.02	0.07	–	0.10	0.08	0.04	0.03	0.03	0.004

<sup>a</sup> Corresponding Canadian Forest FBP System fuel type used in CFFEPS.

<sup>b</sup> Peat is not explicitly considered to be duff, however, it is analogous to duff and falls under this FBP fuel type.

<sup>c</sup> Sample numbers varied among the I-CIMS, Vocus PTR-MS, and Picarro G2401-m measurements; therefore, the reported values represent the maximum number of samples available for each fuel across the three instruments.

<sup>d</sup> NMOC<sub>G</sub> (g kg<sup>-1</sup>) was estimated by applying a 28% increase to the NMOC values following the conversion proposed by Hayden et al. (2022).

## Data availability

Data corresponding to this manuscript have been included herein or are available at the data repository Borealis: <https://doi.org/10.5683/SP3/OGR3J1> (Afroz, 2026).

## 585 Supplement

The supplement related to this article is available online

## Author contributions

590 RA, HS, BHI, SGM, AHM, ST, CL, JJBW, OO, AL, and SNW carried out the experiments, with RA, HS, SGM, AHM, ST, OO, and SNW performed data curation and formal analysis. GM prepared and collected samples and, together with SGM, JO, JL, JA, RZ, SNW, and AC, contributed to the study design. JO and RZ planned and oversaw the laboratory campaign. SGM, AC, JO, JL, JA, RZ, and SNW supervised students and personnel and provided scientific guidance. RMS and CM provided instrumentation, with RMS additionally contributing to the study design. RA and SNW prepared the original draft with contributions from all authors. HS, BHI, SGM, JJBW, AL, GM, RMS, CM, AC, JO, JL, JA, and RZ reviewed and commented on the manuscript.

## Competing interests

At least one of the (co-)authors is a member of the editorial board of Atmospheric Chemistry and Physics.

## 595 Acknowledgements

The authors gratefully acknowledge the Northern Forestry Centre for their significant efforts to prepare for and support the lab campaign.. RA acknowledges financial support from the Alberta Innovates Graduate Student Scholarship (AI GSS). BHI acknowledges the National Sciences and Engineering Research Council of Canada (NSERC) for a graduate

<https://doi.org/10.5194/egusphere-2026-2661>

Preprint. Discussion started: 21 May 2026

© Author(s) 2026. CC BY 4.0 License.



student scholarship and Environment and Climate Change Canada (ECCC) for a graduate student supplement. Thank you to Jack Chen and Debora Griffin at ECCC for useful discussion and for reviewing the manuscript.

## 600 **Financial supports**

The study was funded by the Environmental Damages Fund of the Government of Canada through its Climate Action and Awareness Fund.

## **Copyright statement**

The works published in this journal are distributed under the Creative Commons Attribution 4.0 License. This licence does not affect the Crown copyright work, which is re-usable under the Open Government Licence (OGL). The Creative Commons Attribution 4.0 License and the OGL are interoperable and do not conflict with, reduce or limit each other.

605 © Crown Copyright. His Majesty the King in Right of Canada, as represented by the Minister of the Environment, 2025.



## References

- Abatzoglou, J. T. and Williams, A. P.: Impact of anthropogenic climate change on wildfire across western US forests, *Proc. Natl. Acad. Sci. U.S.A.*, 113, 11 770–11 775, <https://doi.org/10.1073/pnas.1607171113>, 2016.
- Agee, J. K. and Skinner, C. N.: Basic principles of forest fuel reduction treatments, *For. Ecol. Manage.*, 211, 83–96, <https://doi.org/10.1016/j.foreco.2005.01.034>, 2005.
- 610 Akagi, S., Yokelson, R. J., Wiedinmyer, C., Alvarado, M. J., Reid, J. S., Karl, T., Crounse, J. D., and Wennberg, P. O.: Emission factors for open and domestic biomass burning for use in atmospheric models, *Atmos. Chem. Phys.*, 11, 4039–4072, <https://doi.org/10.5194/acp-11-4039-2011>, 2011.
- Alvarado, M. J. and Prinn, R. G.: Formation of ozone and growth of aerosols in young smoke plumes from biomass burning: 1. Lagrangian parcel studies, *J. Geophys. Res. Atmos.*, 114, <https://doi.org/10.1029/2008JD011144>, 2009.
- 615 Amiro, B., Todd, J., Wotton, B., Logan, K., Flannigan, M., Stocks, B., Mason, J., Martell, D., and Hirsch, K. G.: Direct carbon emissions from Canadian forest fires, 1959–1999, *Can. J. For. Res.*, 31, 512–525, <https://doi.org/10.1139/x00-197>, 2001.
- Amiro, B., Cantin, A., Flannigan, M., and De Groot, W.: Future emissions from Canadian boreal forest fires, *Can. J. For. Res.*, 39, 383–395, <https://doi.org/10.1139/X08-154>, 2009.
- 620 Andreae, M. O.: Emission of trace gases and aerosols from biomass burning—an updated assessment, *Atmos. Chem. Phys.*, 19, 8523–8546, <https://doi.org/10.5194/acp-19-8523-2019>, 2019.
- Andreae, M. O. and Merlet, P.: Emission of trace gases and aerosols from biomass burning, *Global biogeochemical cycles*, 15, 955–966, <https://doi.org/10.1029/2000GB001382>, 2001.
- Bertschi, I., Yokelson, R. J., Ward, D. E., Babbitt, R. E., Susott, R. A., Goode, J. G., and Hao, W. M.: Trace gas and particle emissions from fires in large diameter and belowground biomass fuels, *J. Geophys. Res. Atmos.*, 108, <https://doi.org/10.1029/2002JD002100>, 2003.
- 625 Binte Shahid, S., Lacey, F. G., Wiedinmyer, C., Yokelson, R. J., and Barsanti, K. C.: NEIVAv1. 0: Next-generation Emissions Inventory expansion of Akagi et al.(2011) version 1.0, *Geosci. Model Dev.*, 17, 7679–7711, <https://doi.org/10.5194/gmd-17-7679-2024>, 2024.
- Biomass Burning in Canada: Addressing Climate and Air Quality Impacts. <https://bbcan.net/> (last access: 3 March 2026), 2021.
- Boutzis, R. M., Stroud, C. A., Ménard, S., Chen, J., Menelaou, K., Munoz-Alpizar, R., Kornic, D., and Manseau, P. M.: Operational chemical weather forecasting with the ECCC online Regional Air Quality Deterministic Prediction System version 023 (RAQDPS023)-Part 2: Multi-year prospective and retrospective performance evaluation, *EGUsphere* [preprint], <https://doi.org/10.5194/egusphere-2025-4323>, 09 Dec 2025.
- 630 Burling, I., Yokelson, R. J., Griffith, D. W., Johnson, T. J., Veres, P., Roberts, J., Warneke, C., Urbanski, S., Reardon, J., Weise, D., et al.: Laboratory measurements of trace gas emissions from biomass burning of fuel types from the southeastern and southwestern United States, *Atmos. Chem. Phys.*, 10, 11 115–11 130, <https://doi.org/10.5194/acp-10-11115-2010>, 2010.
- 635 Campos, I., Abrantes, N., Pereira, P., Micaelo, A. C., Vale, C., and Keizer, J. J.: Forest fires as potential triggers for production and mobilization of polycyclic aromatic hydrocarbons to the terrestrial ecosystem, *Land Degrad. Dev.*, 30, 2360–2370, <https://doi.org/10.1002/ldr.342>, 2019.
- Canadian Interagency Forest Fire Centre: Canada Report 2016. [https://www.ciffc.ca/sites/default/files/2019-03/2016\\_canada\\_report\\_2017\\_05\\_15\\_02.pdf](https://www.ciffc.ca/sites/default/files/2019-03/2016_canada_report_2017_05_15_02.pdf) (last access : 9 October 2025), 2017.
- Carter, T. S., Heald, C. L., Jimenez, J. L., Campuzano-Jost, P., Kondo, Y., Moteki, N., Schwarz, J. P., Wiedinmyer, C., Darmenov, A. S., da Silva, A. M., et al.: How emissions uncertainty influences the distribution and radiative impacts of smoke from fires in North America, *Atmos. Chem. Phys. Discuss.*, 2019, 1–50, <https://doi.org/10.5194/acp-20-2073-2020>, 2019.
- 640 Chen, J., Anderson, K., Pavlovic, R., Moran, M. D., Englefield, P., Thompson, D. K., Munoz-Alpizar, R., and Landry, H.: The FireWork v2. 0 air quality forecast system with biomass burning emissions from the Canadian Forest Fire Emissions Prediction System v2. 03, *Geosci. Model Dev.*, 12, 3283–3310, <https://doi.org/10.5194/gmd-12-3283-2019>, 2019.
- 645 Chen, L.-W., Verburg, P., Shackelford, A., Zhu, D., Susfalk, R., Chow, J., and Watson, J.: Moisture effects on carbon and nitrogen emission from burning of wildland biomass, *Atmos. Chem. Phys.*, 10, 6617–6625, <https://doi.org/10.5194/acp-10-6617-2010>, 2010.
- Chen, L.-W. A., Moosmüller, H., Arnott, W. P., Chow, J. C., Watson, J. G., Susott, R. A., Babbitt, R. E., Wold, C. E., Lincoln, E. N., and Hao, W. M.: Emissions from laboratory combustion of wildland fuels: Emission factors and source profiles, *Environ. Sci. Technol.*, 41, 4317–4325, <https://doi.org/10.1021/es062364i>, 2007.
- 650 Chen, Q., Zhao, Y., Zheng, B., and Zhang, L.: Unexpected high ammonia emissions from boreal fires in 2021 and 2023, *Geophys. Res. Lett.*, 52, e2024GL112 396, <https://doi.org/10.1029/2024GL112396>, 2025.
- Coggon, M. M., Veres, P. R., Yuan, B., Koss, A., Warneke, C., Gilman, J. B., Lerner, B. M., Peischl, J., Aikin, K. C., Stockwell, C. E., et al.: Emissions of nitrogen-containing organic compounds from the burning of herbaceous and arboraceous biomass: Fuel composition dependence and the variability of commonly used nitrile tracers, *Geophys. Res. Lett.*, 43, 9903–9912, <https://doi.org/10.1002/2016GL070562>, 2016.
- 655



- Copernicus Atmosphere Monitoring Service: Global fire emissions (CAM5 GFAS). <https://atmosphere.copernicus.eu/global-fire-emissions> (last access: 23 December 2025), 2022.
- Cutzen, P. J. and Andreae, M. O.: Biomass burning in the tropics: Impact on atmospheric chemistry and biogeochemical cycles, *science*, 250, 1669–1678, <https://doi.org/10.1126/science.250.4988.1669>, 1990.
- 660 Cubison, M., Ortega, A., Hayes, P., Farmer, D., Day, D., Lechner, M., Brune, W., Apel, E., Diskin, G., Fisher, J., et al.: Effects of aging on organic aerosol from open biomass burning smoke in aircraft and laboratory studies, *Atmos. Chem. Phys.*, 11, 12 049–12 064, <https://doi.org/10.5194/acp-11-12049-2011>, 2011.
- De Gouw, J. and Warneke, C.: Measurements of volatile organic compounds in the earth's atmosphere using proton-transfer-reaction mass spectrometry, *Mass spectrometry reviews*, 26, 223–257, <https://doi.org/10.1002/mas.20119>, 2007.
- 665 De Groot, W., Pritchard, J., and Lynham, T.: Forest floor fuel consumption and carbon emissions in Canadian boreal forest fires, *Can. J. For. Res.*, 39, 367–382, <https://doi.org/10.1139/X08-192>, 2009.
- Dyakonov, A. J., Walker, R. T., Brown, C. A., Perini, F. R., Passer, D. S., Guan, J., and Robinson, E. A.: Studies of the formation of smoke phenols, *Beitr. Tabakforsch. Int.*, 23, 68–84, <https://doi.org/10.2478/cttr-2013-0850>, 2008.
- Forestry Canada, Fire Danger Group: Development and Structure of the Canadian Forest Fire Behaviour Prediction System; Information report ST-X-3. <https://ostr-backend-prod.azure.cloud.nrcan-rncan.gc.ca/server/api/core/bitstreams/c2935183-f5eb-4193-8e6e-30669d0c0614/content> (last access: 23 December 2025), 1992.
- 670 Gilman, J., Lerner, B., Kuster, W., Goldan, P., Warneke, C., Veres, P., Roberts, J., De Gouw, J., Burling, I., and Yokelson, R.: Biomass burning emissions and potential air quality impacts of volatile organic compounds and other trace gases from fuels common in the US, *Atmos. Chem. Phys.*, 15, 13 915–13 938, <https://doi.org/10.5194/acp-15-13915-2015>, 2015.
- 675 Goode, J. G., Yokelson, R. J., Susott, R. A., and Ward, D. E.: Trace gas emissions from laboratory biomass fires measured by open-path Fourier transform infrared spectroscopy: Fires in grass and surface fuels, *J. Geophys. Res. Atmos.*, 104, 21 237–21 245, <https://doi.org/10.1029/1999JD900360>, 1999.
- Goode, J. G., Yokelson, R. J., Ward, D. E., Susott, R. A., Babbitt, R. E., Davies, M. A., and Hao, W. M.: Measurements of excess O<sub>3</sub>, CO<sub>2</sub>, CO, CH<sub>4</sub>, C<sub>2</sub>H<sub>4</sub>, C<sub>2</sub>H<sub>2</sub>, HCN, NO, NH<sub>3</sub>, HCOOH, CH<sub>3</sub>COOH, HCHO, and CH<sub>3</sub>OH in 1997 Alaskan biomass burning plumes by airborne Fourier transform infrared spectroscopy (AFTIR), *J. Geophys. Res. Atmos.*, 105, 22 147–22 166, <https://doi.org/10.1029/2000JD900287>, 2000.
- Government of Canada: Public Safety Canada. Parliamentary Committee Notes: Canadian Wildfires. <https://www.publicsafety.gc.ca/cnt/trnsprnc/brfng-mtrls/prlmntry-bndrs/20240322/16-en.aspx> (last access: 9 October 2025), 2024.
- Government of Canada: Peatland fires and carbon emissions. <https://natural-resources.canada.ca/forest-forestry/wildland-fires/peatland-fires-carbon-emissionsresearch>. (last access: 3 March 2026), 2026.
- 685 Griffin, D., Chen, J., Anderson, K., Makar, P., McLinden, C. A., Dammers, E., and Fogal, A.: Biomass burning CO emissions: exploring insights through TROPOMI-derived emissions and emission coefficients, *Atmos. Chem. Phys.*, 24, 10 159–10 186, <https://doi.org/10.5194/acp-24-10159-2024>, 2024.
- Hatch, L. E., Rivas-Ubach, A., Jen, C. N., Lipton, M., Goldstein, A. H., and Barsanti, K. C.: Measurements of I/SVOCs in biomass-burning smoke using solid-phase extraction disks and two-dimensional gas chromatography, *Atmos. Chem. Phys.*, 18, 17 801–17 817, <https://doi.org/10.5194/acp-18-17801-2018>, 2018.
- 690 Hayden, K. L., Li, S.-M., Liggio, J., Wheeler, M. J., Wentzell, J. J., Leithead, A., Brickell, P., Mittermeier, R. L., Oldham, Z., Mihele, C. M., et al.: Reconciling the total carbon budget for boreal forest wildfire emissions using airborne observations, *Atmos. Chem. Phys.*, 22, 12 493–12 523, <https://doi.org/10.5194/acp-22-12493-2022>, 2022.
- 695 Hecobian, A., Liu, Z., Hennigan, C. J., Huey, L. G., Jimenez, J. L., Cubison, M. J., Vay, S., Diskin, G. S., Sachse, G. W., Wisthaler, A., et al.: Comparison of chemical characteristics of 495 biomass burning plumes intercepted by the NASA DC-8 aircraft during the ARCTAS/CARB-2008 field campaign, *Atmos. Chem. Phys.*, 11, 13 325–13 337, <https://doi.org/10.5194/acp-11-13325-2011>, 2011.
- Hu, Y. and Rein, G.: Development of gas signatures of smouldering peat wildfire from emission factors, *International Journal of Wildland Fire*, 31, 1014–1032, <https://doi.org/10.1071/WF21093>, 2022.
- 700 Hu, Y., Fernandez-Anez, N., Smith, T. E., and Rein, G.: Review of emissions from smouldering peat fires and their contribution to regional haze episodes, *International Journal of Wildland Fire*, 27, 293–312, <https://doi.org/10.1071/WF17084>, 2018.
- Hu, Y., Christensen, E., Restuccia, F., and Rein, G.: Transient gas and particle emissions from smouldering combustion of peat, *Proceedings of the Combustion Institute*, 37, 4035–4042, <https://doi.org/10.1016/j.proci.2018.06.008>, 2019.
- Jaffe, D. A. and Wigder, N. L.: Ozone production from wildfires: A critical review, *Atmos. Environ.*, 51, 1–10, <https://doi.org/10.1016/j.atmo>  
705 *env.2011.11.063*, 2012.
- Jaffe, D. A., O'Neill, S. M., Larkin, N. K., Holder, A. L., Peterson, D. L., Halofsky, J. E., and Rappold, A. G.: Wildfire and prescribed burning impacts on air quality in the United States, *J. Air Waste Manag. Assoc.*, 70, 583–615, <https://doi.org/10.1080/10962247.2020.1749731>, 2020.



- Ji, Y., Huey, L. G., Tanner, D. J., Lee, Y. R., Veres, P. R., Neuman, J. A., Wang, Y., and Wang, X.: A vacuum ultraviolet ion source (VUV-710 IS) for iodide–chemical ionization mass spectrometry: a substitute for radioactive ion sources, *Atmospheric Measurement Techniques*, 13, 3683–3696, <https://doi.org/10.5194/amt-13-3683-2020>, 2020.
- Kaiser, J., Heil, A., Andreae, M., Benedetti, A., Chubarova, N., Jones, L., Morcrette, J.-J., Razinger, M., Schultz, M., Suttie, M., et al.: Biomass burning emissions estimated with a global fire assimilation system based on observed fire radiative power, *Biogeosciences*, 9, 527–554, <https://doi.org/10.5194/bg-9-527-2012>, 2012.
- 715 Kallenborn, R., Halsall, C., Dellong, M., and Carlsson, P.: The influence of climate change on the global distribution and fate processes of anthropogenic persistent organic pollutants, *J. Environ. Monit.*, 14, 2854–2869, <https://doi.org/10.1039/C2EM30519D>, 2012.
- Kleffmann, J.: Daytime sources of nitrous acid (HONO) in the atmospheric boundary layer, *ChemPhysChem*, 8, 1137–1144, <https://doi.org/10.1002/cphc.200700016>, 2007.
- Koppmann, R., Von Czapiewski, K., and Reid, J.: A review of biomass burning emissions, part I: gaseous emissions of carbon monoxide, 720 methane, volatile organic compounds, and nitrogen containing compounds, *Atmos. Chem. Phys. Discuss.*, 5, 10455–10516, <https://doi.org/10.5194/acpd-5-10455-2005>.
- Koss, A. R., Warneke, C., Yuan, B., Coggon, M. M., Veres, P. R., and de Gouw, J. A.: Evaluation of NO<sup>+</sup> reagent ion chemistry for online measurements of atmospheric volatile organic compounds, *Atmos. Meas. Tech.*, 9, 2909–2925, <https://doi.org/10.5194/amt-9-2909-2016>, 2016.
- 725 Koss, A. R., Sekimoto, K., Gilman, J. B., Selimovic, V., Coggon, M. M., Zarzana, K. J., Yuan, B., Lerner, B. M., Brown, S. S., Jimenez, J. L., et al.: Non-methane organic gas emissions from biomass burning: identification, quantification, and emission factors from PTR-ToF during the FIREX 2016 laboratory experiment, *Atmos. Chem. Phys.*, 18, 3299–3319, <https://doi.org/10.5194/acp-18-3299-2018>, 2018.
- Krechmer, J., Lopez-Hilfiker, F., Koss, A., Hutterli, M., Stoermer, C., Deming, B., Kimmel, J., Warneke, C., Holzinger, R., Jayne, J., et al.: Evaluation of a new reagent-ion source and focusing ion–molecule reactor for use in proton-transfer-reaction mass spectrometry, *Analytical 730 chemistry*, 90, 12011–12018, <https://doi.org/10.1021/acs.analchem.8b02641>, 2018.
- Kreider, M. R., Higuera, P. E., Parks, S. A., Rice, W. L., White, N., and Larson, A. J.: Fire suppression makes wildfires more severe and accentuates impacts of climate change and fuel accumulation, *Nat. Commun.*, 15, 2412, <https://doi.org/10.1038/s41467-024-46702-0>, 2024.
- Kuhlbusch, T. A., Lobert, J. M., Crutzen, P. J., and Warneck, P.: Molecular nitrogen emissions from denitrification during biomass burning, *Nature*, 351, 135–137, <https://doi.org/10.1038/351135a0>, 1991.
- 735 Larkin, N. K., Raffuse, S. M., Huang, S., Pavlovic, N., Lahm, P., and Rao, V.: The comprehensive fire information reconciled emissions (CFIRE) inventory: Wildland fire emissions developed for the 2011 and 2014 US National Emissions Inventory, *J. Air Waste Manag. Assoc.*, 70, 1165–1185, <https://doi.org/10.1080/10962247.2020.1802365>, 2020.
- Lin, M., Horowitz, L. W., Hu, L., and Permar, W.: Reactive nitrogen partitioning enhances the contribution of Canadian wildfire plumes to US ozone air quality, *Geophys. Res. Lett.*, 51, e2024GL109369, <https://doi.org/10.1029/2024GL109369>, 2024.
- 740 Lindaas, J., Pollack, I. B., Calahorrano, J. J., O’Dell, K., Garofalo, L. A., Pothier, M. A., Farmer, D. K., Kreidenweis, S. M., Campos, T., Flocke, F., et al.: Empirical insights into the fate of ammonia in western US wildfire smoke plumes, *J. Geophys. Res. Atmos.*, 126, e2020JD033730, <https://doi.org/10.1029/2020JD033730>, 2021a.
- Lindaas, J., Pollack, I. B., Garofalo, L. A., Pothier, M. A., Farmer, D. K., Kreidenweis, S. M., Campos, T. L., Flocke, F., Weinheimer, A. J., Montzka, D. D., et al.: Emissions of reactive nitrogen from Western US wildfires during summer 2018, *J. Geophys. Res. Atmos.*, 126, 745 e2020JD032657, <https://doi.org/10.1029/2020JD032657>, 2021b.
- Link, M. F., Claffin, M. S., Cecelski, C. E., Akande, A. A., Kilgour, D., Heine, P. A., Coggon, M., Stockwell, C. E., Jensen, A., Yu, J., et al.: Product ion distributions using H<sub>3</sub>O<sup>+</sup> proton-transfer-reaction time-of-flight mass spectrometry (PTR-ToF-MS): mechanisms, transmission effects, and instrument-to-instrument variability, *Atmospheric Measurement Techniques*, 18, 1013–1038, <https://doi.org/10.5194/amt-18-1013-2025>, 2025.
- 750 Liu, T., Liu, Q., Li, Z., Huo, L., Chan, M., Li, X., Zhou, Z., and Chan, C. K.: Emission of volatile organic compounds and production of secondary organic aerosol from stir-frying spices, *Sci. Total Environ.*, 599, 1614–1621, <https://doi.org/10.1016/j.scitotenv.2017.05.147>, 2017a.
- Liu, X., Huey, L. G., Yokelson, R. J., Selimovic, V., Simpson, I. J., Müller, M., Jimenez, J. L., Campuzano-Jost, P., Beyersdorf, A. J., Blake, D. R., et al.: Airborne measurements of western US wildfire emissions: Comparison with prescribed burning and air quality implications, *J. 755 Geophys. Res. Atmos.*, 122, 6108–6129, <https://doi.org/10.1002/2016JD026315>, 2017b.
- Los Gatos Research: H<sub>2</sub>S/NH<sub>3</sub> Analyzer. <https://www.yodify.com/Products/WXYooZ/www.yodify.com/Products/WXYooZ/H-S-NH-Analyzer> (last access: 26 December 2025), 2025.
- Majluf, F. Y., Krechmer, J. E., Daube, C., Knighton, W. B., Dyroff, C., Lambe, A. T., Fortner, E. C., Yacovitch, T. I., Roscioli, J. R., Herndon, S. C., et al.: Mobile near-field measurements of biomass burning volatile organic compounds: Emission ratios and factor analysis, *Environ. 760 Sci. Technol. Lett.*, 9, 383–390, <https://doi.org/10.1021/acs.estlett.2c00194>, 2022.



- Miller, D. J., Sun, K., Zondlo, M. A., Kanter, D., Dubovik, O., Welton, E. J., Winker, D. M., and Ginoux, P.: Assessing boreal forest fire smoke aerosol impacts on US air quality: A case study using multiple data sets, *J. Geophys. Res. Atmos.*, 116, <https://doi.org/10.1029/2011JD016170>, 2011.
- Mohr, C., Lopez-Hilfiker, F. D., Zotter, P., Prévôt, A. S., Xu, L., Ng, N. L., Herndon, S. C., Williams, L. R., Franklin, J. P., Zahniser, M. S., et al.: Contribution of nitrated phenols to wood burning brown carbon light absorption in Detling, United Kingdom during winter time, *Environ. Sci. Technol.*, 47, 6316–6324, <https://doi.org/10.1021/es400683v>, 2013.
- 765 Moore, B., Thompson, D. K., Schroeder, D., Johnston, J. M., and Hvenegaard, S.: Using infrared imagery to assess fire behaviour in a mulched fuel bed in black spruce forests, *Fire*, 3, 37, <https://doi.org/10.3390/fire3030037>, 2020.
- Moraes, A. H., Talebian, S., Afroz, R., Al-Jabiri, M. H., Chan, A. W. H., Chang, R. Y.-W., Chen, K., Corbin, J. C., Drinovec, L., Isenor, B. H., Lee, A., Liggio, J., Liu-Kang, C., Marshall, G., Moallemi, A., Mocnik, G., Moussa, S. G., Olfert, O., Saleh, M., Sipkens, T. A., Shen, H., Wentzell, J. J. B., Wren, S. N., Yus-Díez, J., Hayes, P. L., Abbatt, J. P. D., Olfert, J., and Zhao, R.: Combustion Characteristics and Emission Factors of Trace Gases and Particulate Matter from Biomass Relevant to Canadian Wildfires: Overview of the 2024 BBCan Campaign, *ESS Open Archive [preprint]*, <https://doi.org/10.22541/essoar.15002871/v1>, 7 May 2026.
- 770 Natural Resources Canada: How much forest does Canada have? <https://natural-resources.canada.ca/forest-forestry/state-canada-forests/much-forest-does-canada-have>. (last access: 9 October 2025), 2025a.
- Natural Resources Canada: Canadian Wildland Fire Information System, FBP Fuel Type Descriptions. <https://cwfis.cfs.nrcan.gc.ca/background/fueltypes/c> (last access: 23 December 2025), 2025b.
- Pagonis, D., Krechmer, J. E., De Gouw, J., Jimenez, J. L., and Ziemann, P. J.: Effects of gas-wall partitioning in Teflon tubing and instrumentation on time-resolved measurements of gas-phase organic compounds, *Atmospheric measurement techniques*, 10, 4687–4696, <https://doi.org/10.5194/amt-10-4687-2017>, 2017.
- 780 Pan, X., Ichoku, C., Chin, M., Bian, H., Darmenov, A., Colarco, P., Ellison, L., Kucsera, T., da Silva, A., Wang, J., et al.: Six global biomass burning emission datasets: intercomparison and application in one global aerosol model, *Atmos. Chem. Phys.*, 20, 969–994, <https://doi.org/10.5194/acp-20-969-2020>, 2020.
- Patil Shirish, S., Kelkar Tushar, S., and Bhalerao Satish, A.: Mulching: A soil and water conservation practice, *Res. J. Agric. For. Sci.*, 2320, 6063, 2013.
- 785 Permar, W., Wang, Q., Selimovic, V., Wielgasz, C., Yokelson, R. J., Hornbrook, R. S., Hills, A. J., Apel, E. C., Ku, I.-T., Zhou, Y., et al.: Emissions of trace organic gases from Western US wildfires based on WE-CAN aircraft measurements, *J. Geophys. Res. Atmos.*, 126, e2020JD033838, <https://doi.org/10.1029/2020JD033838>, 2021.
- Randerson, J., van der Werf, G., Giglio, L., Collatz, G., and Kasibhatla, P.: Global fire emissions database, version 3.1, ORNL DAAC, <https://doi.org/10.3334/ORNLDAAC/1191>, 2013.
- 790 Rein, G.: Smouldering fires and natural fuels, *Fire phenomena and the Earth system: an interdisciplinary guide to fire science*, pp. 15–33, <https://doi.org/10.1002/9781118529539.ch2>, 2013.
- Rein, G., Cleaver, N., Ashton, C., Pironi, P., and Torero, J. L.: The severity of smouldering peat fires and damage to the forest soil, *Catena*, 74, 304–309, <https://doi.org/10.1016/j.catena.2008.05.008>, 2008.
- 795 Riva, M., Pospisilova, V., Frege, C., Perrier, S., Bansal, P., Jorga, S., Sturm, P., Thornton, J. A., Rohner, U., and Lopez-Hilfiker, F.: Evaluation of a reduced-pressure chemical ion reactor utilizing adduct ionization for the detection of gaseous organic and inorganic species, *Atmospheric Measurement Techniques*, 17, 5887–5901, <https://doi.org/10.5194/amt-17-5887-2024>, 2024.
- Roberts, J. M., Stockwell, C. E., Yokelson, R. J., De Gouw, J., Liu, Y., Selimovic, V., Koss, A. R., Sekimoto, K., Coggon, M. M., Yuan, B., et al.: The nitrogen budget of laboratory-simulated western US wildfires during the FIREX 2016 Fire Lab study, *Atmos. Chem. Phys.*, 20, 8807–8826, <https://doi.org/10.5194/acp-20-8807-2020>, 2020.
- 800 Rogers, H. M., Ditto, J. C., and Gentner, D. R.: Evidence for impacts on surface-level air quality in the northeastern US from long-distance transport of smoke from North American fires during the Long Island Sound Tropospheric Ozone Study (LISTOS) 2018, *Atmos. Chem. Phys.*, 20, 671–682, <https://doi.org/10.5194/acp-20-671-2020>, 2020.
- Romanias, M., Coggon, M., Fatima, A., Burkholder, J., Dagaut, P., Decker, Z., Warneke, C., Stockwell, C., Roberts, J., Tomas, A., et al.: Emissions and Atmospheric Chemistry of Furanoids from Biomass Burning: Insights from Laboratory to Atmospheric Observations, *ACS Earth Space Chem.*, 8, 857–899, <https://doi.org/10.1021/acsearthspacechem.3c00226>, 2024.
- 805 Seinfeld, J. H. and Pandis, S. N.: *Atmospheric chemistry and physics: from air pollution to climate change*, John Wiley & Sons, 3rd edn., ISBN 1119221166, 2016.
- Sekimoto, K., Koss, A. R., Gilman, J. B., Selimovic, V., Coggon, M. M., Zarzana, K. J., Yuan, B., Lerner, B. M., Brown, S. S., Warneke, C., et al.: High-and low-temperature pyrolysis profiles describe volatile organic compound emissions from western US wildfire fuels, *Atmos. Chem. Phys.*, 18, 9263–9281, <https://doi.org/10.5194/acp-18-9263-2018>, 2018.
- 810



- Selimovic, V., Yokelson, R. J., Warneke, C., Roberts, J. M., De Gouw, J., Reardon, J., and Griffith, D. W.: Aerosol optical properties and trace gas emissions by PAX and OP-FTIR for laboratory-simulated western US wildfires during FIREX, *Atmos. Chem. Phys.*, 18, 2929–2948, <https://doi.org/10.5194/acp-19-3905-2019>, 2018.
- 815 Selimovic, V., Yokelson, R. J., McMeeking, G. R., and Coefield, S.: In situ measurements of trace gases, PM, and aerosol optical properties during the 2017 NW US wildfire smoke event, *Atmos. Chem. Phys.*, 19, 3905–3926, <https://doi.org/10.5194/acp-19-3905-2019>, 2019.
- Simon, H., Beck, L., Bhawe, P. V., Divita, F., Hsu, Y., Luecken, D., Mobley, J. D., Pouliot, G. A., Reff, A., Sarwar, G., et al.: The development and uses of EPA's SPECIATE database, *Atmospheric Pollution Research*, 1, 196–206, <https://doi.org/10.5094/APR.2010.026>, 2010.
- Simpson, I. J., Akagi, S., Barletta, B., Blake, N., Choi, Y., Diskin, G., Fried, A., Fuelberg, H., Meinardi, S., Rowland, F., et al.: Boreal forest fire 820 emissions in fresh Canadian smoke plumes: C 1-C 10 volatile organic compounds (VOCs), CO<sub>2</sub>, CO, NO<sub>2</sub>, NO, HCN and CH<sub>3</sub>CN, *Atmos. Chem. Phys.*, 11, 6445–6463, <https://doi.org/10.5194/acp-11-6445-2011>, 2011.
- Sommers, W. T., Loehman, R. A., and Hardy, C. C.: Wildland fire emissions, carbon, and climate: Science overview and knowledge needs, *For. Ecol. Manage.*, 317, 1–8, <https://doi.org/10.1016/j.foreco.2013.12.014>, 2014.
- Stockwell, C., Yokelson, R., Kreidenweis, S., Robinson, A., DeMott, P., Sullivan, R., Reardon, J., Ryan, K., Griffith, D., and Stevens, L.: Trace 825 gas emissions from combustion of peat, crop residue, domestic biofuels, grasses, and other fuels: configuration and Fourier transform infrared (FTIR) component of the fourth Fire Lab at Missoula Experiment (FLAME-4), *Atmos. Chem. Phys.*, 14, 9727–9754, <https://doi.org/10.5194/acp-14-9727-2014>, 2014.
- Stockwell, C., Veres, P., Williams, J., and Yokelson, R.: Characterization of biomass burning emissions from cooking fires, peat, crop residue, and other fuels with high-resolution proton-transfer-reaction time-of-flight mass spectrometry, *Atmos. Chem. Phys.*, 15, 845–865, <https://doi.org/10.5194/acp-15-845-2015>, 2015.
- 830 Stockwell, C. E., Jayarathne, T., Cochrane, M. A., Ryan, K. C., Putra, E. I., Saharjo, B. H., Nurhayati, A. D., Albar, I., Blake, D. R., Simpson, I. J., et al.: Field measurements of trace gases and aerosols emitted by peat fires in Central Kalimantan, Indonesia, during the 2015 El Niño, *Atmos. Chem. Phys.*, 16, 11 711–11 732, <https://doi.org/10.5194/acp-16-11711-2016>, 2016.
- Stutz, J., Oh, H.-J., Whitlow, S. I., Anderson, C., Dibb, J. E., Flynn, J. H., Rappenglück, B., and Lefter, B.: Simultaneous DOAS and mist- 835 chamber IC measurements of HONO in Houston, TX, *Atmos. Environ.*, 44, 4090–4098, <https://doi.org/10.1016/j.atmosenv.2009.02.003>, 2010.
- Teledyne: Nox analyzer (N500, Teledyne API). <https://www.teledyne-api.com/en-us/products/n500> (last access: 23 December 2025), 2025.
- Thompson, D., Wotton, B., and Waddington, J.: Estimating the heat transfer to an organic soil surface during crown fire, *Int. J. Wildland Fire*, 24, 120–129, <https://doi.org/10.1071/WF12121>, 2015.
- 840 Thompson, D. K., Schroeder, D., Wilkinson, S. L., Barber, Q., Baxter, G., Cameron, H., Hsieh, R., Marshall, G., Moore, B., Refai, R., et al.: Recent crown thinning in a boreal black spruce forest does not reduce spread rate nor total fuel consumption: results from an experimental crown fire in Alberta, Canada, *Fire*, 3, 28, <https://doi.org/10.3390/fire3030028>, 2020.
- Turetsky, M., Wieder, K., Halsey, L., and Vitt, D.: Current disturbance and the diminishing peatland carbon sink, *Geophys. Res. Lett.*, 29, 21–1, <https://doi.org/10.1029/2001GL014000>, 2002.
- 845 Turetsky, M. R., Kane, E. S., Harden, J. W., Ottmar, R. D., Manies, K. L., Hoy, E., and Kasischke, E. S.: Recent acceleration of biomass burning and carbon losses in Alaskan forests and peatlands, *Nat. Geosci.*, 4, 27–31, <https://doi.org/10.1038/ngeo1027>, 2011.
- Turetsky, M. R., Benscotter, B., Page, S., Rein, G., Van Der Werf, G. R., and Watts, A.: Global vulnerability of peatlands to fire and carbon loss, *Nat. Geosci.*, 8, 11–14, <https://doi.org/10.1038/ngeo2325>, 2015.
- Urbanski, S.: Wildland fire emissions, carbon, and climate: Emission factors, *For. Ecol. Manage.*, 317, 51–60, <https://doi.org/10.1016/j.foreco.2013.05.045>, 2014.
- 850 Urbanski, S. P., Long, R. W., Halliday, H., Lincoln, E. N., Habel, A., and Landis, M. S.: Fuel layer specific pollutant emission factors for fire prone forest ecosystems of the western US and Canada, *Atmos. Environ.: X*, 16, 100 188, <https://doi.org/10.1016/j.aeaoa.2022.100188>, 2022.
- USEPA: Health effects of wildfire smoke. <https://www.airnow.gov/sites/default/files/2021-05/wildfire-smoke-guide-revised-2019-chapters-1-3.pdf>. (last access: 9 October 2025), 2019.
- 855 Voulgarakis, A. and Field, R. D.: Fire influences on atmospheric composition, air quality and climate, *Current Pollution Reports*, 1, 70–81, <https://doi.org/10.1007/s40726-015-0007-z>, 2015.
- Voulgarakis, A., Marlier, M. E., Faluvegi, G., Shindell, D. T., Tsigaridis, K., and Mangeon, S.: Interannual variability of tropospheric trace gases and aerosols: The role of biomass burning emissions, *J. Geophys. Res. Atmos.*, 120, 7157–7173, <https://doi.org/10.1002/2014JD022926>, 860 2015.
- Wang, X., Gu, R., Wang, L., Xu, W., Zhang, Y., Chen, B., Li, W., Xue, L., Chen, J., and Wang, W.: Emissions of fine particulate nitrated phenols from the burning of five common types of biomass, *Environ. Pollut.*, 230, 405–412, <https://doi.org/10.1016/j.envpol.2017.06.072>, 2017.



- Ward, D. and Radke, L.: Emissions measurements from vegetation fires: A comparative evaluation of methods and results, in: In: Crutzen, PJ; Goldammer, JG, eds. *Fire in the Environment: The Ecological, Atmospheric, and Climatic Importance of Vegetation Fires*. Dahlem Workshop Reports: Environmental Sciences Research Report 13. Chichester, England: John Wiley & Sons. p. 53-76., pp. 53–76, 1993.
- 865 Watson, J. G., Cao, J., Chen, L.-W. A., Wang, Q., Tian, J., Wang, X., Gronstal, S., Ho, S. S. H., Watts, A. C., and Chow, J. C.: Gaseous, PM 2.5 mass, and speciated emission factors from laboratory chamber peat combustion, *Atmos. Chem. Phys.*, 19, 14 173–14 193, 14173–14193. <https://doi.org/10.5194/acp-19-14173-2019>, 2019.
- Westerling, A. L., Hidalgo, H. G., Cayan, D. R., and Swetnam, T. W.: Warming and earlier spring increase western US forest wildfire activity, *science*, 313, 940–943, <https://doi.org/10.1126/science.1128834>, 2006.
- 870 Wiedinmyer, C., Kimura, Y., McDonald-Buller, E. C., Emmons, L. K., Buchholz, R. R., Tang, W., Seto, K., Joseph, M. B., Barsanti, K. C., Carlton, A. G., et al.: The Fire Inventory from NCAR version 2.5: an updated global fire emissions model for climate and chemistry applications, *Geosci. Model Dev.*, 16, 3873–3891, <https://doi.org/10.5194/gmd-16-3873-2023>, 2023.
- Wilkinson, S., Moore, P., Thompson, D., Wotton, B. M., Hvenegaard, S., Schroeder, D., and Waddington, J. M.: The effects of black spruce fuel 875 management on surface fuel condition and peat burn severity in an experimental fire, *Can. J. For. Res.*, 48, 1433–1440, <https://doi.org/10.1139/cjfr-2018-0217>, 2018.
- Xiong, Y., Du, K., and Huang, Y.: One-third of global population at cancer risk due to elevated volatile organic compounds levels, *npj Clim. Atmos. Sci.*, 7, 54, <https://doi.org/10.1038/s41612-024-00598-1>, 2024.
- Yokelson, R. J., Griffith, D. W., and Ward, D. E.: Open-path Fourier transform infrared studies of large-scale laboratory biomass fires, *J. Geophys. Res. Atmos.*, 101, 21 067–21 080, <https://doi.org/10.1029/96JD01800>, 1996.
- 880 Yokelson, R. J., Susott, R., Ward, D. E., Reardon, J., and Griffith, D. W.: Emissions from smoldering combustion of biomass measured by open-path Fourier transform infrared spectroscopy, *J. Geophys. Res. Atmos.*, 102, 18 865–18 877, <https://doi.org/10.1029/97JD00852>, 1997.
- Yokelson, R. J., Christian, T. J., Karl, T., and Guenther, A.: The tropical forest and fire emissions experiment: laboratory fire measurements and synthesis of campaign data, *Atmos. Chem. Phys.*, 8, 3509–3527, <https://doi.org/10.5194/acp-8-3509-2008>, 2008.
- 885 Yokelson, R. J., Burling, I., Gilman, J., Warneke, C., Stockwell, C., De Gouw, J., Akagi, S., Urbanski, S., Veres, P., Roberts, J., et al.: Coupling field and laboratory measurements to estimate the emission factors of identified and unidentified trace gases for prescribed fires, *Atmos. Chem. Phys.*, 13, 89–116, <https://doi.org/10.5194/acp-13-89-2013>, 2013.
- Young, C. J., Joudan, S., Tao, Y., Wentzell, J. J., and Liggio, J.: High time resolution ambient observations of gas-phase perfluoroalkyl carboxylic acids: implications for atmospheric sources, *Environ. Sci. Technol. Lett.*, 11, 1348–1354, <https://doi.org/10.1021/acs.estlett.4c00897>, 2024.
- 890 Zhan, J., Feng, Z., Liu, P., He, X., He, Z., Chen, T., Wang, Y., He, H., Mu, Y., and Liu, Y.: Ozone and SOA formation potential based on photochemical loss of VOCs during the Beijing summer, *Environ. Pollut.*, 285, 117 444, <https://doi.org/10.1016/j.envpol.2021.117444>, 2021.